Ecological Indicators 133 (2021) 108453

Contents lists available at ScienceDirect

Ecological Indicators

journal homepage: www.elsevier.com/locate/ecolind

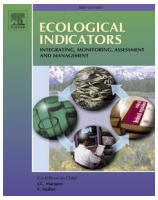

Spatio-temporal characteristics and determinants of anthropogenic nitrogen and phosphorus inputs in an ecologically fragile karst basin: Environmental responses and management strategies

Guoyu Xu [a,b,c,1], Jie Xiao [a,b,1], David M. Oliver [e], Zhiqi Yang [c,d], Kangning Xiong [a,*], Zhongming Zhao [f], Lilin Zheng [g], Hongxiang Fan [b], Fuxiang Zhang [b,c]

[a] School of Karst Science / State Engineering Technology Institute for Karst Desertification Control, Guizhou Normal University, Guiyang 550001, China
[b] Key Laboratory of Watershed Geographic Sciences, Nanjing Institute of Geography and Limnology, Chinese Academy of Sciences, Nanjing 210008, China
[c] University of Chinese Academy of Sciences, Beijing 100049, China
[d] Key Laboratory of Regional Sustainable Development Modeling, Institute of Geographic Sciences and Natural Resources Research, Chinese Academy of Sciences, Beijing 100101, China
[e] Biological & Environmental Sciences, Faculty of Natural Sciences, University of Stirling, Stirling FK9 4LA, UK
[f] Department of Geography, King's College London, London, UK
[g] Key Laboratory of Geographic Information Science (Ministry of Education), School of Geographic Sciences, East China Normal University, Shanghai 200241, China

ARTICLE INFO

Keywords:
NANI&NAPI
Temporal-temporal heterogeneity
The Grid fractal dimension
Environment responses
Geographical detector model
Determinant analysis

ABSTRACT

Excessive nitrogen and phosphorus inputs to land and subsequent export to water via runoff leads to aquatic ecosystem deterioration. The WRB is the world's largest karst basin which is characterized by a fragile ecosystem coupling with high population pressure, and the transformation of intensive agriculture. Quantifying different sources of pollution in karst regions is challenging due to the complexity of landscape topography and geology coupled with high transmissivity and connectivity of subsurface hydrological systems. This results in large uncertainty associated with nitrogen (N) and phosphorus (P) flow pathways. This combination of factors contributes to the WRB being a high priority for quantitatively understanding the contribution of regional nutrient inputs and those of other major water quality determinants. Here we applied the latest statistical data (2000–2018) and simple quasi-mass-balance methods of net anthropogenic nitrogen and phosphorus inputs (NANI and NAPI) to estimate spatio-temporal heterogeneity of N and P inputs. The results show that while NANI and NAPI are first decreasing, this is followed by an increasing trend during 2000–2018, with average values of 11262.06 ± 2732 kg N km^{-2} yr^{-1} and 2653.91 ± 863 kg P km^{-2} yr^{-1} respectively. High N and P concentrations in the river drainage network are related to the spatial distribution of excessive inputs of N and P. Rapid urbanization, livestock farming and the conflicts between economic development and lagged-environmental management are the main reasons for the incremental regional N and P inputs. Management decisions on nutrient pollution in karst regions need careful consideration to reduce ecological impacts and contamination of karst aquifers. This study provides new insight for policy and decision making in the WRB, highlighting policy options for managing nutrient inputs and providing recommendations for closing the science-policy divide.

1. Introduction

Nitrogen (N) and phosphorus (P) are limiting nutrients, providing an indispensable role to support the functions and processes that operate within dynamic natural ecosystems (Guignard et al., 2017; Vitousek and Howarth, 1991). The ubiquitous availability of cheap synthetic fertilizers, explosive growth of fossil fuels and high stocking rates of livestock have resulted in patterns of N and P use becoming increasingly inefficient and dissipative. For example, the reactive N flux imposed to the Earth system by anthropogenic dominating inputs has soared to more than 180 Tg N $year^{-1}$, far exceeding the N fixed by natural processes (Fowler et al., 2013). Phosphorus flows in the environment have

* Corresponding author.
E-mail address: xiongkn@gznu.edu.cn (K. Xiong).
[1] The two authors contributed equally to this work and should be considered co-first authors.

https://doi.org/10.1016/j.ecolind.2021.108453
Received 13 August 2021; Received in revised form 3 December 2021; Accepted 5 December 2021

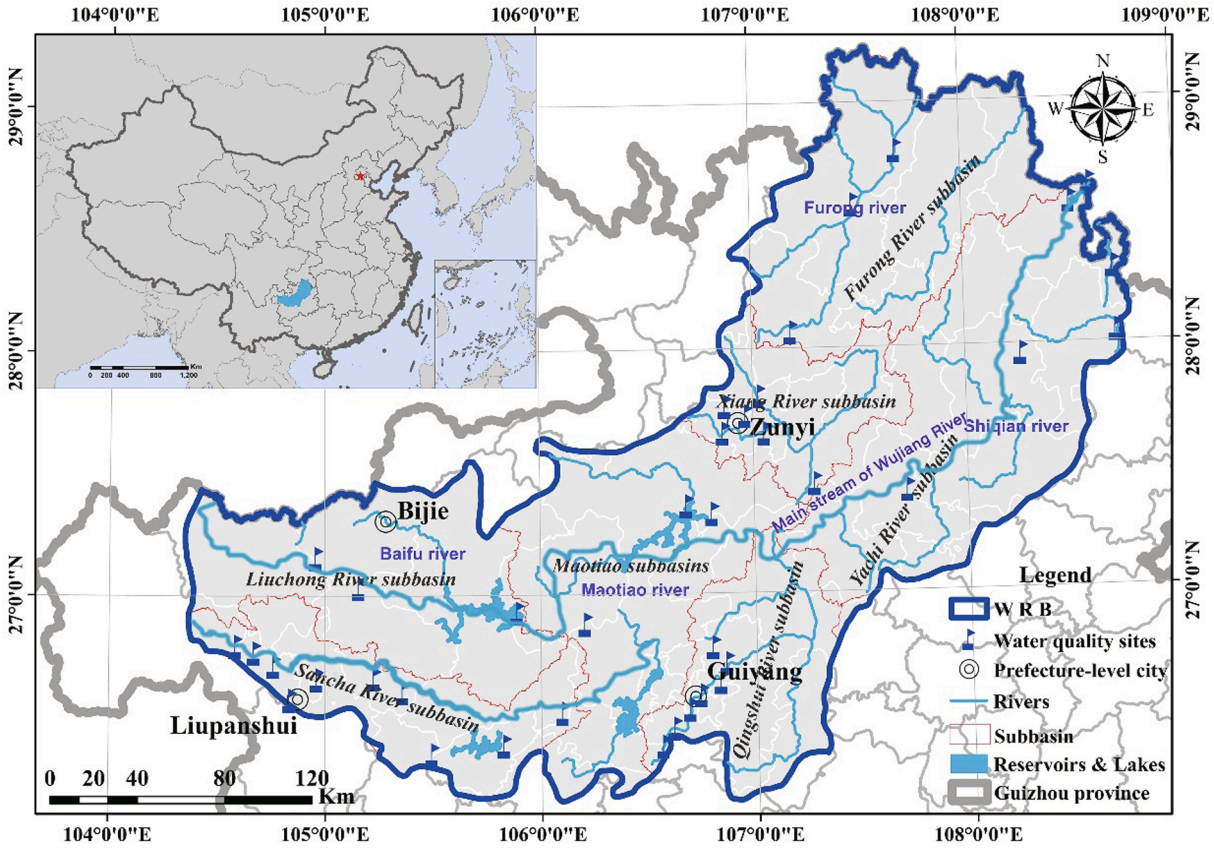

Fig. 1. Boundaries of WRB.

accelerated four-fold over the past six decades (Nesme et al., 2018). N and P cycles in the Earth system have therefore been distorted by human activity, which have exceeded the so-called"planetary boundary" (MacDonald et al., 2011; Scholz and Wellmer, 2013; Steffen et al., 2015). In turn, global aquatic ecosystems have suffered irreversible cascade effects, such as eutrophication of surface waters (Carpenter, 2005), toxic algal blooms (Brooks et al., 2016; Rabalais, 2002), low dissolved oxygen (Diaz, 2001), and loss of aquatic biodiversity (Allan et al., 2020). Differences in catchment characteristics of global rivers can result in varying contributions of N and P to aquatic systems from multiple sources, with their spatio-temporal characteristics determined by, e.g., hydrology, climate change, population density, land–use and sewage treatment technology (Seitzinger et al., 2005; Vilmin et al., 2018).

Karst is a globally distributed landscape occupying approximately 15% of the Earth's ice-free continent area, accommodating 20% of the world's population and contributing to 50% or more of regional freshwater supplies (Ford and Williams, 2007; Chen et al., 2017; Hartmann et al., 2014). The WRB is situated in typical of subtropical regions and the world's largest continuous karst landscape. Uneven seasonal distribution and high frequency of heavy rainfall is coupled with fragile karst landscape features e.g., steep terrains and thin, easily erodible soils with low natural vegetation cover, which often leads to land degradation. Improper land use practices (cropping on sloping land and overgrazing) can accelerate rocky desertification, which is considered a major environmental hazard and an obstacle to the development of agriculture. Indeed, declines in soil productivity force the expansion of farmland to less suitable land, e.g., edge of slopes and ridges, which exacerbate the mobilization and transport of anthropogenic N and P from land to rivers, lakes and open waters (Powers et al., 2016; Sinha and Michalak, 2016).

The WRB is experiencing multiple stressors from population increase, the decoupling between crop production and import-dependent livestock production, industrial structure changes and dam construction, all of which have increased over the last two decades. According to the water quality report from the Environmental Protection Bureau of Guizhou Province, more than 60% of rivers in the WRB fail to reach the required water quality level (Class IV). A dual isotopic approach has also demonstrated that nitrate pollution of groundwater in the WRB is derived from fertilizers, livestock manures and wastewater sources due to the high permeability of the karstified zone below the soil (Li et al., 2021a; Zeng et al., 2020; Wang et al., 2019; Hartmann et al., 2015). Determining the components of N and P loading in complex and heterogeneous landscapes is therefore an important stage of nutrient management planning because it can help to pinpoint the primary sources of pollution for targeted alleviated strategies (Jean-Olivier et al., 2016).

Physical process-based models e.g., SWAT, AGNPS, HSPF can simulate nutrient cycling and pathways with high accuracy but require numerous parameters in the fitting process (Arhonditsis et al., 2007; Hashemi et al., 2016; Ding et al., 2010; Mayorga et al., 2010; Singh et al., 2005). Furthermore, in karst basins, the complex subsurface system is comprised of karst pipelines, caves and fissures, which can facilitate the leakage of surface water to groundwater resulting in high uncertainty with respect to unknown nutrient flow pathways (Song et al., 2019; Fiorillo et al., 2015; Jiang et al., 2014). There is also much uncertainty in model parameterization or inadequate observational data to support calibration and validation, which further hinders the application of process-based models in karst watersheds (Hartmann et al., 2015; Malagò et al., 2016; Fiorillo et al., 2015; Li et al., 2021b). Based on mass balance, the Net Anthropogenic Nitrogen Inputs (NANI) (Howarth et al., 1996) and Net Anthropogenic Phosphorus Inputs (NAPI) models (Russell et al., 2008) are one of the most widely adopted conceptual approaches used around the world for estimating nutrient budgets, which can be established for a region without using an intricate N and P

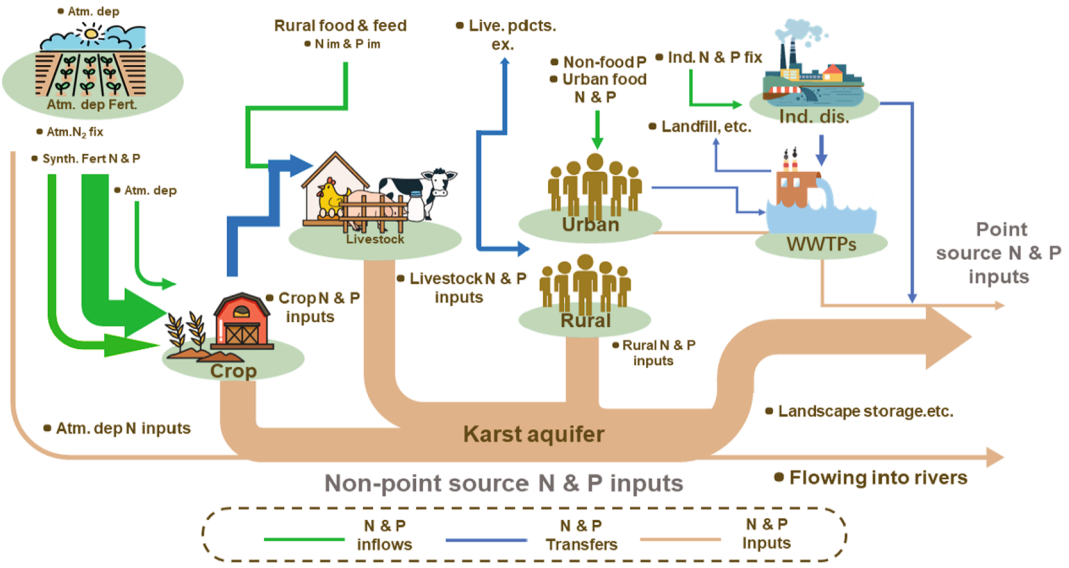

Fig. 2. Material flow conceptual diagram for anthropogenic nitrogen and phosphorus inputs estimation.

model (Han and Allan, 2008; Russell et al., 2008; Sobota et al., 2013; Swaney et al., 2015). NANI and NAPI can therefore unequivocally evaluate regional sources of N and P and their variations at different temporal and spatial scales, which helps to inform environmental management approaches to minimize environmental pollution around the world (Metson et al., 2017; Goyette et al., 2019). NANI and NAPI calculations can be modified to suit varying features for different regions of the world and differences in data accessibility and availability (Hong et al., 2012; Goyette et al., 2016; Swaney et al., 2015).

Excessive Human-induced N and P inputs that result in environment degradation in ecologically fragile areas clearly warrants investigation. In response, studies have investigated correlations between N and P loads and socioeconomic factors including e. g., population, societal policy, per capita GDP, urbanization, diet choice, and energy consumption (Cui et al., 2021a; Sinha et al., 2019). A variety of methods have been applied to study factors governing N and P pollution, such as Logarithmic Mean Divisia Index LMDI (Gao et al., 2015) and Redundancy Analysis RDA (Cui et al., 2021c); however, the Geographical Detector Method (GDM), proposed by Wang et al. (2010) has rarely been used. The GDM does not need a linear hypothesis to reveal the driving factors behind spatial stratified heterogeneity. Thus, if the values of two variables have similar geographical distribution and are spatially correlated, the interactive influences of these factors can be detected and high intercorrelations among two or more independent variables need not be considered (Wang et al., 2010).

The overarching aim of this study, therefore, was to use socio-economic data and apply the NANI/NAPI methods to quantify long-term (2000–2018) nutrient budgets at a county scale in the WRB. Then, we utilized GDM to analyze the power of determinants for each driving factor according to data and findings from previous studies to inform the driving factors for NANI and NAPI. In addition, we used grid fractal dimension to investigate spatial responses in the water environment to NANI and NAPI, with the results providing new information to support decision-makers and stakeholders responsible for environmental management in such ecologically fragile areas.

2. Materials and methods

2.1. Study area

The WRB (105°36′30″-105°46′30″E, 25°39′13″~25°41′00″N) is located in Guizhou province and plays an important role of an ecological security barrier for maintaining the ecosystem balance and biodiversity in the Yangtze River Basin (Fig. 1). It covers a total area of 80300 km^2 and runs 1037 km in length from west to east. The WRB experiences a subtropical humid monsoon climate with an average annual temperature of 13 ~ 18℃ and average annual precipitation between 800 and 1600 mm. Cultivated land, grassland, and forest are the three dominant land use types in the WRB. The whole basin is typical of mixed-land-use paddy farming in the karst areas of south China with approximately half of the land used for growing crops such as rice, rapeseed, maize, soybeans and fruits and vegetables.

The WRB provides agricultural irrigation, urban development, river navigation and other functions for more than 35 million people in 54 counties in Guizhou Province. The population density has an extremely high heterogeneity from 78 to 1048 people/km^2 in 2015, with a decreasing trend in population density from southwest to northeast (Cheng and Li, 2020). The WRB has high social, economic and ecological importance and is considered as a key transportation hub to the economic hinterland of Southwest China. A large cascade hydropower station had been built in the WRB, which has changed local biogeochemical cycles and elevated the accumulation of nutrients in reservoirs (Kunz et al., 2011; Harrison et al., 2009). There have been several reports about the retention effects of cascade reservoirs on nutrient elements, which may also influence biodiversity and promote eutrophication in rivers (Yang et al., 2020). In the past ten years, owing to strict farmland protection policies, the percentage of cropland areas in the WRB remains stable although construction has been increasing along with fertilizer use and more livestock has been raised to feed a more affluent and growing human population. As described above, the water environment situation in WRB faces a huge crisis.

2.2. Data resources

Social and economic data sets including crop yields, fertilizer use, livestock density, and population and GDP are derived from Prefectural Bureau of Statistics and the Agricultural Census in Guizhou province, the Statistical Bulletin of national economic and social development, and the 13th and 14th five-year plan in Guizhou province. Data on point wastewater discharge was provided by the first (in 1995) and second (in 2015) pollution census in Guizhou province. Missing data within our long-term dataset was estimated using linear interpolations (Hong et al., 2017). The atmospheric deposition raster format data sets in 1995 and 2015 were available open access from the Regional Emission inventory in China with a spatial resolution of 1 km (Yu et al., 2019a) http://www.sciencedb.cn /dataSet/handle/607htm). Land use data for 2015 was

Table 1
Calculation of each nitrogen and Phosphorus source.

Items	Non-point source inputs calculation methods	Description	Items	Point source inputs calculation methods	Description
$NANI_n$/ $NAPI_n$	$NANIn = Nchem + Nfix + Ndep + Nr - im$ (2) $N_{chem}$is the amount of N in N synthetic ertilizer application; N_{fix} is th sum of symbiotic N in crop N fixation by cultivation of legume crops and non-symbiotic N fixation in agricultural ecosystem); N_{dep}represents the amount of atmospheric ntrogen deposition (N_{Oy}) (Howarth et al., 2012); $N_{R\text{-}im}$ is defined as total N consumption (by livestock and humans) minus total N production (by crops and livestock) (Schaefer et al., 2009). $NAPIn = Pfet + Pnon + PR - im$ (4) P_{fer} is Phosphorus content in P fertilizers; P_{non} refers to the phosphorus containing detergent used for household cleaning; $P_{R\text{-}im}$ is the total P consumption (by livestock and humans) minus total P production (by crops and livestock)	This method refers Zhang et al. (2019b).	$NANI_p$/ $NAPI_p$	$NANIp = (Nind + Nurban)(1 - IsewIrem - tn)$ (3) N_{ind} referred to the product of industrial sewage effluent flow; $N_{urban}$was estimated as the product of urban population and average nitrogen consumption per capita;I_{sew} is the percentage of sewage discharged from the treatment plants; $I_{rem\text{-}tn}$ is the average N processing rate by a sewage plant. $NANIp = (Pind + Purban)(1 - IsewIrem - tp)$ (5) P_{ind} is the amount of phosphorus in industrial wastewater; P_{urban} is the amount of phosphorus in urban domestic wastewater; $I_{rem\text{-}tp}$ is the average P processing rate by a sewage plant.	This method proposed by Zhang et al. (2019b).
N_{chem} / P_{chem}	$Nchem = Nf + (Cf \times 32\%)$ (6) $N_f$is the N content in yearly N fertilizer application; C_f is the N content in yearly N fertilizer application consumption of fertilizers. $Pchem = Pf \times P2O5 \times 436.4$ (7) P_f is P fertilizer application to kg P by multiplying by 436.4 kg P per ton P_2O_5 applied.	An average N and P content of 32% of compound fertilizer in China (Zhang et al., 2009).	N_{ind} / P_{ind}	W_{ind} is $NInd = WInd \times 25$ (8) $PInd = WInd \times 2$ (9) the amount of industrial sewage.	We use the parameters reported in YZB to evaluated the industrial N discharge (25 mg/L) and Industrial P discharge (2 mg/L), respectively (Yang et al., 2003).
N_{fix}	$Nfix = Nsfix + Nnon - sfix$ (10) Nsfixand Nnon-sfix were symbiotic N fixation (leguminous crops, soybean and peanut).	Relevant coefficients are shown in Supplementary material (ST1)	N_{urban} / P_{urban}	$NUrban = WUrban \times 4.77$ (11) $PUrban = WUrban \times 0.52$ (12) W_{urban} refer to the population in urban region.	The average N emission (4.77 kg N yr^{-1}) and average P emission 0.52kgP yr^{-1}per capita by urban inhabitant of China was refered respectively (Han et al., 2014; Han et al., 2013; Jing et al., 2008)
Pnon	$Pnon = Wurban \times 1.6$ (13) Wurban refer to the population in urban region; 1.6 refer to Non food phosphorus consumption coefficient.	FNPSC (2010)	I_{sew}	$I_{rem\text{-}tn}$ refer to average reported value of 0.6 referred to (zhang et al., 2019b)	According to the research results of Qiu et al. (2010) the average removal rate
N_{dep}	We defined as the NO_y comes considered as a regional input of nitrogen.	The data of atmospheric nitrogen deposition derived from Yu et al. (2019a)	$I_{rem\text{-}tn}$	Irem-tp was set at 0.7(Zhang et al., 2019b)	According to the research results of Qiu et al. (2010) the average removal rate
$N_{R\text{-}im}$ / $P_{R\text{-}im}$	$NR - im = Nrural + Nanimal - Ncrop - Npro$ (14) N_{rural}和N_{animal} were the food nitrogen consumption of rural residents and livestock and poultry respectively; N_{crop} refers to nitrogen in crops; N_{pro} was the nitrogen content of animal products $PR - im = Prural + Panimal - Pcrop - Ppro$ (15) P_{rural} and P_{animal} were the food phosphorus consumption of rural residents and livestock and poultry respectively P_{crop} refers to phosphorus in crops; P_{pro} was the phosphorus content of animal products.	Relevant conversion coefficients are shown in Supplementary materials (ST2-3)	$I_{rem\text{-}tp}$		

Note: The units are kg N km^{-2} yr^{-1} and kg P km^{-2} yr^{-1}. *Nr-im* and *Pr-im* are allowed to be negative.

provided by the Resources and Environmental Science Data Center, Chinese Academy of Sciences (http://www.resdc.cn/). Monthly water quality data from 2000 to 2018, including Ammonium (NH_4^+-N), total phosphorus (TP) and total nitrogen (TN) at 38 water monitoring sites were acquired from the Environmental Protection Bureau of Guizhou province in accordance with the national environmental quality standards for surface water (GB3838-2002).

2.3. System principle of NANI and NAPI calculation

The NANI / NAPI model has been developed over many years, enabling modifications to model structure, estimation methods and scale transformation methods (Cui et al., 2021b; Hong et al., 2013; Schaefer et al., 2009). We estimated NANI and NAPI according to the approach developed by Zhang et al. (2019c), whose methods differentiate point and non-point sources in NANI and NAPI while establishing a black box linking anthropogenic production and consumption processes, which removes traditional material flow analysis and its complex process. The computational hypothesis of the whole-process is represented as a mass flow via four stages I-Ⅳ (Fig. 2). Namely (I) crop production, (II) livestock consumption, and then into (III) human consumption, and finally into water after (IV) waste treatment. Stage I assumes that rural residents get their nutrition from local livestock products and crops system. The nutritional intake of urban residents mainly depends on food import; on the basis of differences in N and P intake between livestock and crops, N and P imports for food and feed in rural areas are estimated. Industrial N and P pollution originate from industrial sources. Nutrients removed from sewage treatment plants are completely removed and/or buried. In addition, the net input of N and P from food/feed by city dwellers is usually metabolized and excreted by humans and animals, which is then discharged to a sewage treatment plant as domestic sewage. Anthropogenic N and P inputs include (a) atmospheric deposition N, (b) chemical fertilizer inputs, (c) net human and feed import, (d) biological fixation (e) point source wastewater (f) non-food inputs of P, etc.

Eq. (1) and Table 1 show the calculation formulas. More details about the calculation framework and parameters for NANI and NAPI are provided in supplementary material SFig. 2 and ST1-3.

$$\begin{aligned} NANI &= NANIn + NANIp \\ NAPI &= NAPIn + NAPIp \end{aligned} \tag{1}$$

2.4. Grid fractal dimension method

In fractal theory, fractals occupy space efficiently and imply that the self-organizing evolution of geographic systems is governed by some implicit rules that reveal its dynamic mechanism (Frankhauser, 1998; Garg et al., 2014). Grid dimension usually reflects the equilibrium of points in a spatial region, and therefore it is most frequently used to describe fractals and represents an important parameter describing spatial phenomena (Frankhauser, 1998). By analyzing the spatial distribution characteristics of water pollution (inferior water quality) in the river drainage system (TN, NH_4-N and TP above class III) using point elements, the environmental pollution condition can be detected (Deng et al., 2021). Indeed, studies have identified that nutrient flux in waterbodies correlates strongly with spatial homogeneity with NANI and NAPI (Swaney et al., 2015; Martínez-Sabater et al., 2019; Zhang et al., 2020; Russell et al., 2008). The specific grid fractal dimension approach we used is outlined in the following steps:

First, each side of a rectangular area generated by fish net tools was cut up by K equal parts and the whole area was then divided into K^2 grid cell in Arcgis 10.2. The grids that are occupied by point elements $N(\varepsilon)$ in which water quality exceeds class III, followed by the size of the grid ε. D_0 and ε respectively illustrate the capacity dimension and the size of a grid cell ($\varepsilon = 1/k$). Capacity dimension (D_0) and information dimension (D_I) are both considered as the main practical grid dimensions (D).

Second, if the distribution of point elements of inferior water quality is scale-free, they have the following relationship:

$$N(\varepsilon) \propto \varepsilon^{D_0} \tag{16}$$

According to the formula of capacity dimension, $D0 = \lim_{\varepsilon \to 0} \frac{lnN(\varepsilon)}{ln(1/\varepsilon)}$ and ratio mentioned above, When $\varepsilon \to 0$, the following equation holds:

$$lnN(\varepsilon) \approx -D0 ln\varepsilon = D0 ln(1/\varepsilon) \tag{17}$$

where it is assumed that the inferior water quality sampling points are uniform fractals. Next, grids are identified with number i in line and number j in column, and the user sets the number of point elements of " inferior water quality " as N_{ij}, and N as the size of grid cell. The probability of a point element dropping into the i, j_{th} grid cell can be defined as $Pij = \frac{Nij}{N}$, then, $I(\varepsilon)$ the information (information entropy of point elements in the spatial distribution on all grid cells) is calculated as follows:

$$\mathrm{I}(\varepsilon) = -\sum_{i}^{k}\sum_{j}^{k} Pij(\varepsilon) lnPij(\varepsilon) \tag{18}$$

In this formula, $k = \frac{1}{\varepsilon}$ is the number of sections on each side of the study area, if the points of inferior water quality are fractal, there should be $I(\varepsilon) = I0 - D1 ln\varepsilon$. I_0 is a constant and D_I is the information dimension. Then, by performing regression analysis (a least-squares fit), the equations of D_1 and D_0 for the inferior water quality points spatial distributed are obtained. After processing the linear regression of lnK and $ln(\varepsilon)$, the slope of the line represents the capacity dimension D_0. In general, the capacity dimension D_0 is not equal to the information dimension D_I, and the relationship between them is as follows: $D_I < D_0 <$ d, which indicates complexity in the spatial distribution of point elements (Ford and Blenkinsop, 2008; Deng et al., 2021).

2.5. Geographical detector model (GDM)

Geo Detector is primarily used to detect spatial differentiation and analyze the corresponding determinants based on stratified spatial heterogeneity (Wang et al., 2010). The GDM model comprises four detectors according to their specific analytical functions: risk detector, ecological detector, interactive detector and factor detector (Wang et al., 2016). The factor detector was used to identify which social and agricultural factors represent the dominant driving factors of the NANI and NAPI. Factor detector of GDM can quantitatively evaluate the importance of determinants to the dependent variable (Wang et al., 2017) and can be calculated as follows:

$$\mathrm{PD} = 1 - \frac{\sum_{h=1}^{L} Nh\sigma_h^2}{N\sigma^2} = 1 - \frac{SSW}{SST} \tag{19}$$

where q is defined as the power of determinant affecting NANI and NAPI; N_h is the number of units of stratum h, $h = 1,2,\ldots, h$; $N_\sigma{}^2$ and N_h σ_h^2represent global variance in the entire study area and variance in stratum $_i$ respectively; SSW and SST refer to the total variance within stratum and across the region. Normally, q ∈ [0,1], represents the power of determinants and evaluates the relationship between y and x. The software code is freely available at (http://www.sssampling. org/Excel/ Geo detector/).

3. Results and discussions

3.1. Temporal variations and different components of NANI and NAPI

Over time, across the whole basin of 54 counties, the intensities of NANI and NAPI have increased from approximately 8772.55 ± 2351 kg N km^{-2} yr^{-1} and 2021.07 ± 757 kg P km^{-2} yr^{-1} in 2000 to 11262.06 ± 2732 kg N km^{-2} yr^{-1} and 2653.91 ± 863 kg P km^{-2} yr^{-1} in 2018 (See

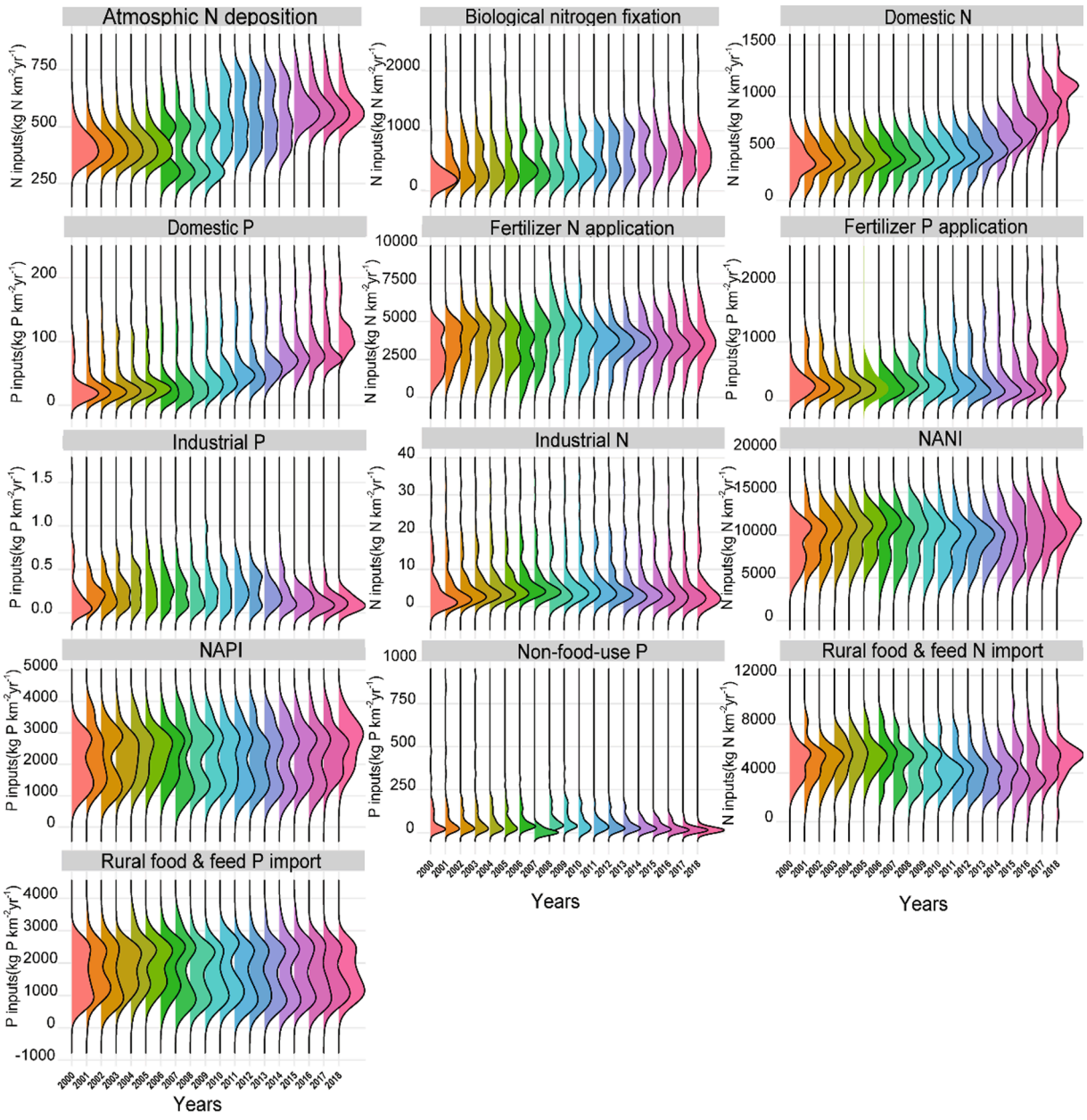

Fig. 3. Ridge plots indicating the variation of each component of NANI(eg. Atmospheric N deposition, Domestic N, Fertilizer N application, Industrial N, Rural food&feed N import, Biological nitrogen fixation, NANI Units: kg N km^{-2} yr^{-1}) and NAPI (Fertilizer P application, Industrial P, Rural food&feed P import, Pnon-food-use, NAPI Units: kg P km^{-2} yr−1) over time across 54 counties of the WRB from 2000 to 2018. Each color in X-axis presents a year during our study period. The Y-axis presents the range of values for each component of NANI and NAPI."

Fig. 3). The relationship between NANI ($R^2 = 0.27$, $p < 0.05$) and NAPI ($R^2 = 0.31$, $p < 0.05$) over time follows a strong linear fit function. Steady increases in NANI and NAPI for the WRB were evident since 2000. However, before 2009, the increase of N and P input showed a small fluctuation and the coefficients of variation (CV) of N and P input were 0.261 and 0.375, respectively. From 2010 onward, the N and P loads increased at a relatively stable rate. Overall, NANI and NAPI in the WRB are currently 2-fold (Han et al., 2014) and 5-fold higher for N and P, respectively, relative to average values for mainland China (Han et al., 2013).

By analyzing the contribution of different NANI and NAPI resources, we found that non-point sources were instrumental in driving the variation of N and P loads, accounting for more than 96% of both the N and P loadings in the WRB (see Fig. 3). Agricultural production, especially livestock farming, plays a crucial part in driving changes in NANI and NAPI. Net imports of N and P in food/feed and fertilizer N and P applications are the two dominant sources of both non-point source N and P loads, which are composed of 45.57% and 67.12 % of N and 81.13% and 46.12% of P input sources, respectively. Fertilizer use experienced a period of rapid growth from 2000 to 2009, but the growth has slowed since 2010, as have crop yields.

Though fertilizer N and P application catalyzed the growth of crop production supply at a much faster rate, animal feed continued to grow since 2009 and net imports of N and P in feed and food represent increasing trends in almost all counties of the WRB (see Fig. 3). Thus, local food/feed is mainly dependent on imports and highlights a lack of self-sufficiency in the WRB. Biological nitrogen fixation is the third dominant source for N inputs, and follows a stable but increasing trend over time. The mean annual biological N fixation is 540.79 ± 339 kg N km − 2 yr − 1. However, the WRB has been promoting urbanization and

the area of urban land use has increased eight-fold from 2000 to 2018.

Atmospheric N deposition is also a major source of anthropogenic net N input, and the mean annual N deposition is 486.82 ± 122 kg N km^{-2} yr^{-1}. Atmospheric N deposition represents a rapid growth from 2010 onward (see Fig. 3). Overall, during our study period, we found large fluctuations in contributions from point-source pollution. The direct discharge of untreated industrial wastewater effluents and domestic wastewater represented the dominant source of point sources of N and P, which accounts for 96% and 97% of contributions, respectively (see Figs. 4 and 5). Domestic wastewater emissions show an increasing trend with time, which is mainly due to China's implementation of urban–rural integration. The urban registered population is increasing but the overall rate of population growth is slowing down (Ye and Christiansen, 2009). In contrast, industrial effluent discharge shows a declining trend with time. Due to lags in environmental management in early stages of economic development in Guizhou province, major sewage treatment plants were mostly concentrated in first-level cities in Guizhou province, of which there were just 7 in the WRB. But, as China further promoted the ecological civilization campaign which facilitated a series of remediation measures (e.g. the construction of wastewater treatment plants) to alleviate pollution from point and diffuse sources, Guizhou province has established sewage treatment plants in every county-level city since 2009 and so the number of sewage treatment plants reached 78 within just over a decade (Tong et al., 2020). Furthermore, the proportion of urban wastewater being treated in Guizhou province increased from 33% in 2000 to 91% in 2015, substantially abating the direct discharge of domestic wastewater to the rivers.

3.2. Spatial heterogeneity and hot spots of anthropogenic N and P inputs

The spatial distribution and dynamics of point and non-point N and P loads in three census years of 2000, 2010, and 2018 across all counties of the WRB were determined (See Fig. 4). Both NANI and NAPI had high intensity inputs, but significant spatial variability across different

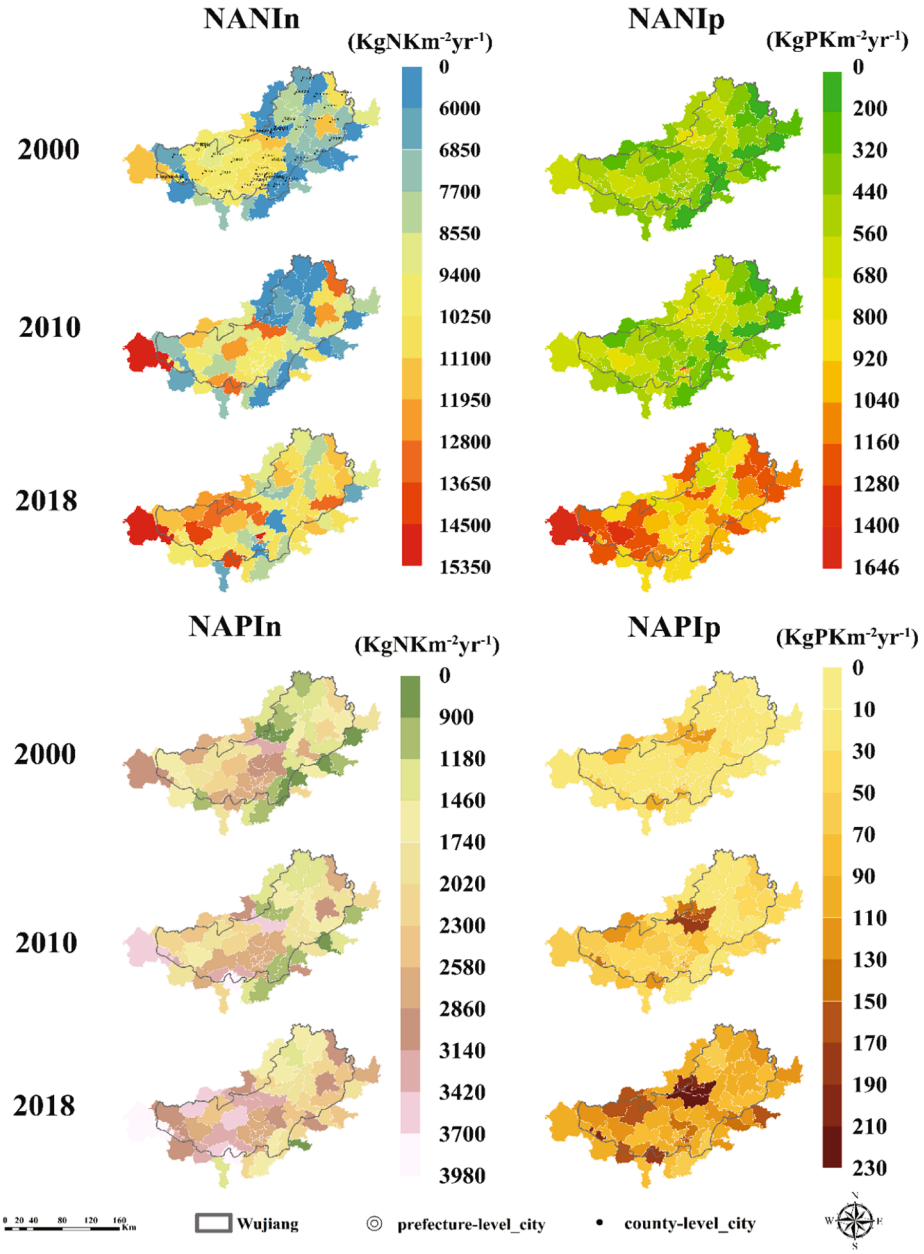

Fig. 4. The spatial distribution of non-point (NANIn and NAPIn) and point (NANIp and NAPIp) nitrogen and phosphorus loads in 54 counties of the WRB for 2000, 2010 and 2018, respectively.

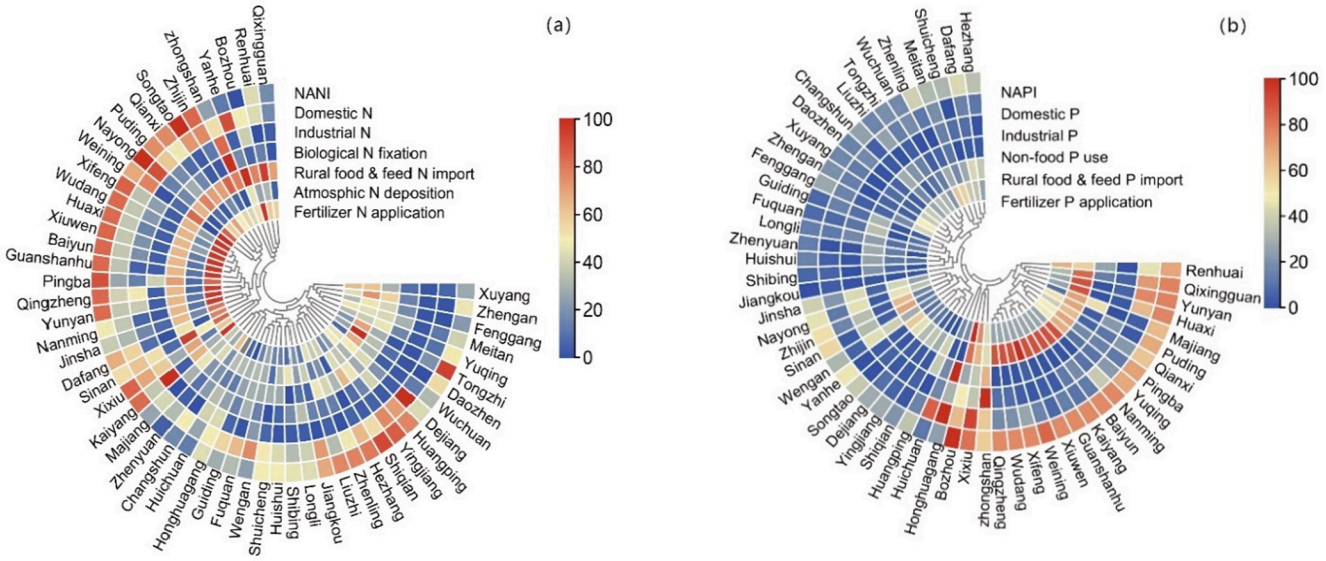

Fig. 5. Percentage increase in N loads (a) and P loads (b) from 2000 to 2018 across 54 counties of the WRB.

watersheds in response to different geographical characteristics of the WRB was evident. The upper reaches of the WRB account for 23.1% of the total basin area, and N and P inputs account for 18.9% and 18.1% of the total basin inputs, respectively. The middle reaches accounted for 46.3% of the whole basin area, while N and P input across this region accounted for 53.8% and 57.4% of the whole basin inputs, respectively. The downstream reaches accounted for 30.6% of the whole area, and N and P input accounted for 27.3% and 24.5% of inputs across this region (see Fig. 4). The larger cities of Bijie and Liupanshui are situated in the northwestern upper reaches. Guiyang is in the central region of the middle reaches of the WRB, and Zunyi is in the northeastern region of the middle reaches of the WRB. Population density is much higher close to these urban centers. Overall, due to the intensive activities of agricultural production, such as crop planting and livestock and poultry farming producing a large amount of N and P, upstream and middle reaches record the highest N and P input, which also conform with the spatial patterns of population density. The population density in the downstream areas is sparsely distributed relative to widespread woodland, and large cities are rare in these areas resulting in little industrial wastewater or sewage influx to receiving waters.

As illustrated in the heat maps (see Fig. 5), hotspots of NANI and NAPI occur in the middle reaches of the WRB, where the percentage increase rates for N and P loads from 2000 to 2018 exceed 87.8% and 61.7%, respectively. The three sub-basins: the lower reaches of the WRB subbasin, Xiangriver sub-basin and Maotiao sub-basin have the highest overall increase rate. For non-point sources, the increase in N and P inputs was primarily a result of increasing food & feed N and P imports and increases in fertilizer N and P loads. The resulting hotspots are found in the XR sub-basin and the lower reaches of WRB sub-basins; these locations are termed the 'rice bowl' of the WRB with very flat terrain - which have extensive arable land and abundant grassland. The hotspot areas of biological N fixation were dispersed and generally found in counties promoting ecological restoration of rocky desertification and the development of ecological products and enterprises. The growth rate of biological N fixation is rapid, ranging from 20.2% to 50.7 %, which might become a new source of N. The growth may also be related to the planting N-fixing crops in karst areas as an ecological engineering approach to ensure soil fertility and control rocky desertification (Wang et al., 2019). Increases in atmospheric deposition are mainly in the northeast region of the middle reaches and the southwest region of the upper reaches, which accommodate greater coverage of cultivated land, and are likely derived from agricultural sources (emissions from agricultural machinery and fuel oils) (Yu et al., 2019a). Increases of non-food P were mainly driven by the densely populated counties of the watershed. Similarly, the hot spot areas of industrial waste water P discharge were mainly concentrated in these counties and in the Liuchong-subbasin, which aligns with the distribution of phosphate ore processing factories.

3.3. *The social and economic driving forces for analysis of NANI and NAPI*

To investigate the power of determinants on N and P pollution, the Geographical Detector Model (GDM) was used. Here we examined the effects of 8 indicators on NANI and NAPI by the means of GDM. We applied a Natural Breaks classification method to preprocess the data, which included socioeconomic factors such as urbanization rate (UR), population density (PD), industrial sewage treatment rate (IST) and gross domestic Product (GDP), and agricultural sources factors: fertilizers (Fert), the percentage area of cropland (CA), grain yield (GY), total livestock (TL) during the study period of 2000 to 2018. We take the year of 2000 for example, see our supplemental materials (SFig. 3). By performing GDM, the value of (q) was computed and q values of all the variables were significant at 1% level ($p < 0.01$).

Further detail concerning q values across all years are provided in Fig. 6 and SFig. 4 and SFig. 5. The mean q values for cropland, total livestock, fertilizer application and population density determined for our study period are relatively high; GY, GDP, UR and IST recorded lower mean q values. PD recorded the smallest interquartile range, and spatial heterogeneity of N and P pollution was explicitly accounted for via population factors that dominated over the long-term, see Fig. 6. TL, FERT and CA also recorded relatively narrow interquartile ranges. Data relating to GDP, ISW and GY were highly variable and revealed unstable or fluctuating trends regarding their influences on N and P inputs. Changes over time of PD and CA during the period of 2000 to 2018 represented a gradual rise followed by a declining trend. Long-term upward trends in data existed for TL, FERT, URB and STR (Fig. 6, SFig. 4 and SFig. 5).

For agricultural source factors, the percent of cropland, total livestock and fertilizers contributed clear impacts for NANI and NAPI compared to other driving factors. The q values for cropland, total livestock and fertilizers ranged from 0.325 to 0.658 (CA), 0.401 to 0.658 (TL) and 0. 363 to 0.434 (Fert) in the WRB (SFig. 4 to SFig. 5). Land use, especially cultivated land, is a strong anthropogenic activity indicator,

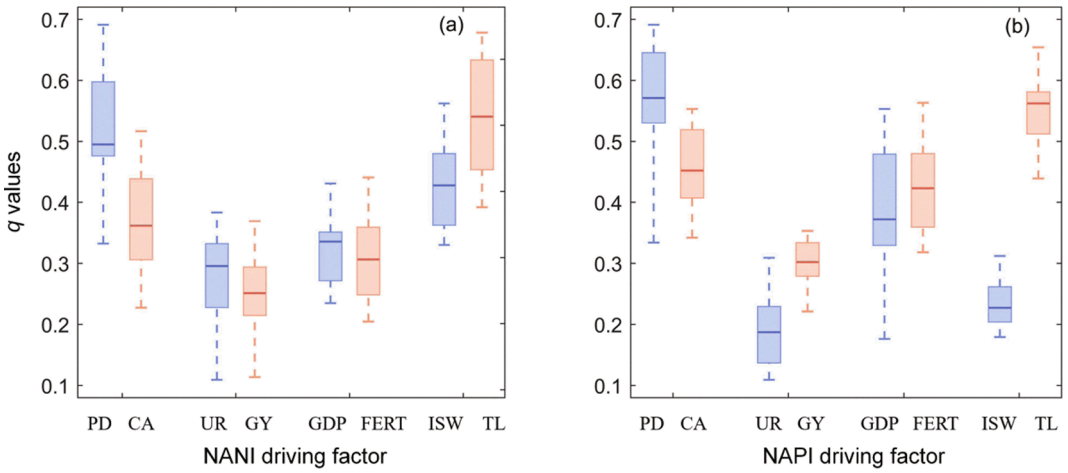

Fig. 6. Box-whisker plot of q values for determinant of NANI and NAPI over 2000 to 2018.

which promotes nutrient cycling and influences N and P pollution of waters (Huang et al., 2014; Porter et al., 2013). In the WRB, the area of arable land accounts for 32% of the basin, representing an extremely high proportion of land use (SFig. 1), but cultivated land resources in Guizhou province are highly distributed and generally of poor quality. However, due to the mild and humid climate, conditions are suitable for livestock husbandry (cattle and sheep). Indeed, a large number of livestock are raised in the WRB in order to meet local food consumption. Compared to a mixed crop-animal production system typical of the plains, livestock husbandry in mountainous areas is far more dispersed across the landscape. The separation between crop and livestock production is an important driver of agricultural nutrient surpluses in the WRB, with excess N and P often in areas of high livestock density. Manures from ruminants and non-ruminants cannot be recycled fully from farmland, which largely increases dependency on imported fertilizer and results in a decoupling between agricultural production and animal feed.

Relative to other social driving factors, population density and urbanization contributed to prominent impacts on N and P pollution in the WRB and generated a q value ranging from 0.425 to 0.658 and 0.351 to 0.343, respectively see SFig. 4 to SFig. 5. The total population of the WRB has increased by about 3 million in the past 20 years according to the sixth and seventh population census. Population explosion can cause a series of biochemical and physical disturbances to the hydrological system. The conversion of different land cover areas is a prime example, especially increases of agricultural and construction land. Urbanization further promotes the rapid centralization of population, resources and economics, but it also increases the potential risks of point source and non-point source pollution (Regmi and Dyck, 2001a). Furthermore, the expansion of impervious surfaces in urban areas may reduce infiltration of surface water and has a key impact on surface runoff dynamics (Walsh et al., 2005). In addition, river burying and lake reclamation aimed at promoting agricultural development can lead to a sharp reduction in surface water availability (Deng et al., 2016). Simultaneously, with the promotion of urbanization and economic development, the demand for water resources for human consumption interacts with water consumption rates for irrigation and water needs for industry, in turn impacting on runoff and pollution input to rivers (Walsh et al., 2005). Both urbanization and economic development can also have significant impacts on food consumption patterns (Regmi and Dyck, 2001b). In addition, dense population and urbanization lead to more Nr emissions in this basin, a pattern consistent across many regions of China still dominated by combustion of fossil fuels. Atmospheric deposition currently follows an increasing linear trend that is predicted to continue due to the energy demands needed to support both urban development and increasing agricultural production. Further, ISW and GY dictate a fluctuating effect on N and P pollution and from the year of 2015, the influence of these two factors begins to decline. GDP per capita is known to align with aspects of environmental degradation and the effects follow a pattern that changes over time. Many studies recognise that GDP follows an inverted U-curve relationship with environmental degradation, supported by an established theoretical hypothesis in the domain of sustainable development: the Environmental Kuznets Curve (EKC) (Marsiglio et al., 2016). Over the period of our study, there was a substantial increase in GDP. The q value of GDP ranges from 0.302 to 0.127 (SFig. 4 and SFig. 5), indicating a significant impact on NANI and NAPI. The q values of GDP mirror an incremental influence of determinants on NANI and NAPI, highlighting an increasing marginal effect of GDP on nutrient pollution.

3.4. *Results of grid fractal dimension and environmental responses to anthropogenic nitrogen and phosphorus inputs*

We examined the relationship of TN, NH_4-N and TP concentrations and NANI and NAPI inputs to the WRB. We believe rivers have received increasing N fluxes from enhanced NANI and NAPI inputs. NANI and NAPI produce a linear relationship with concentrations of TN (R^2 = 0.24), NH4-N (R^2 = 0.50) and TP (R^2 = 0.27) ($p < 0.0001$), which indicates significant impact of NANI and NAPI on water quality (Fig. 7). There is clear evidence of high spatial correlation between the deteriorated water quality data that exceeds standards of grade III of TN, NH4 + -N and TP in the major water quality monitoring sections and the hotspots of NANI and NAPI (average values from 2000 to 2018) across the WRB (see Figs. 4 and 7).

According to the fractal grid dimension results, both information dimension and capacity dimension of water quality indices have a wide scale-free interval (see Fig. 8 and ST5-6). Within a certain measurement scale (scale-free interval), the system conforms to the mathematical meaning of fractal dimension, and fractal dimension does exist. Theoretically speaking, the grid value varies between 0 and 2, which reflects the balance of distribution of water quality exceeding standard points in the regional detection section. When $D_0 = 2$, it indicates that all the water quality exceeds the standard and so concentrates at one point. Normally $1 < D_0 < 2$, thus the larger D_0 is, the more concentrated the spatial equilibrium of various elements of the system, and vice versa. The coefficient of determination diverges from 0.92 to 0.98, which demonstrates significant structural fractal characteristics in space. D_0 is the capacity dimension, the value of which ranges from 1.245 to 1.324 (Fig. 10), manifesting that these points (inferior water quality) are consistent with the geographic line of population distribution and topography. Further analysis showed that the over-standard points of TN, NH_4-N and TP were mainly distributed in the upper and middle

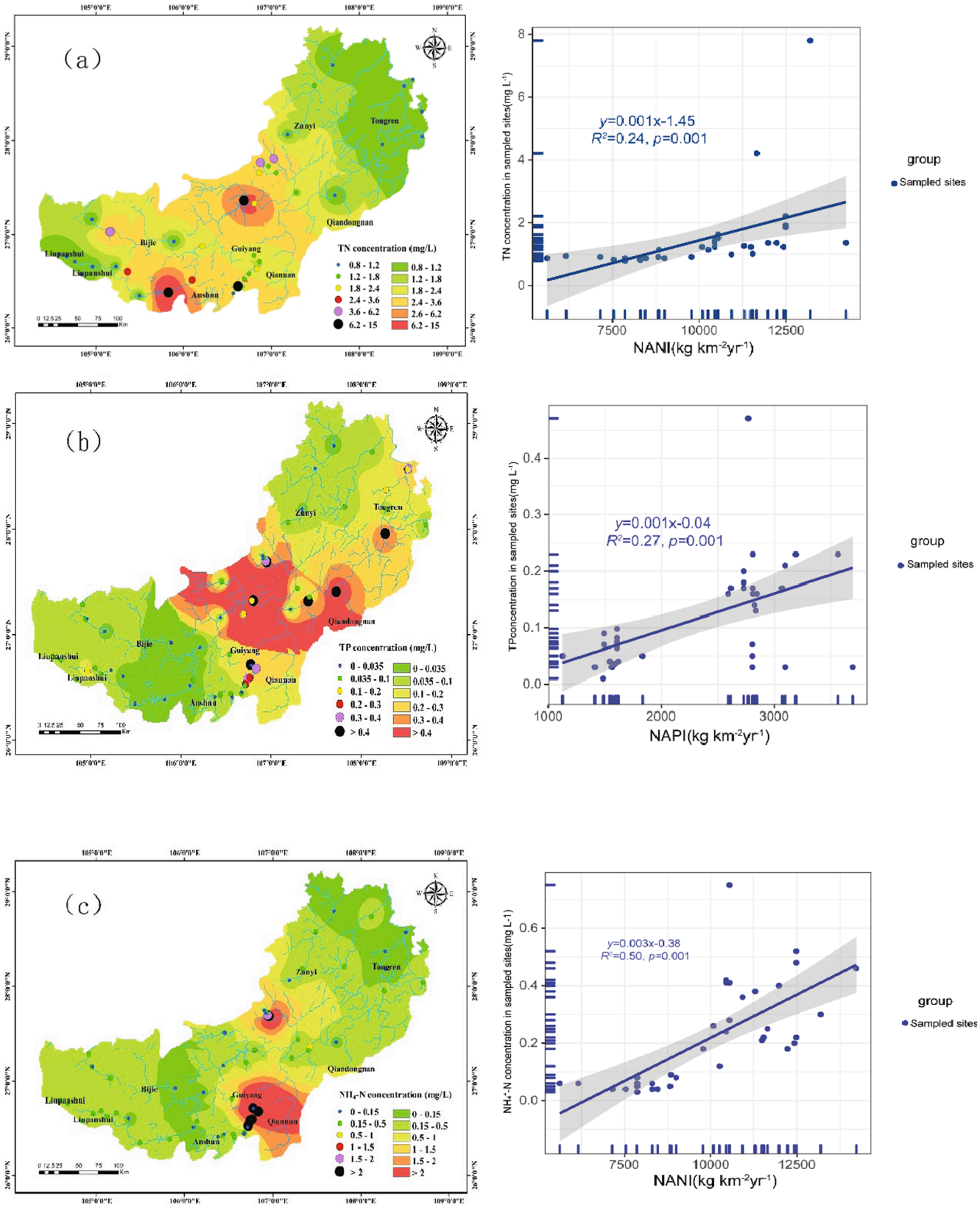

Fig. 7. Spatial density distribution of water quality monitoring sections with TN (a), TP (b) and NH_4-N (c) exceeding grade III standards.

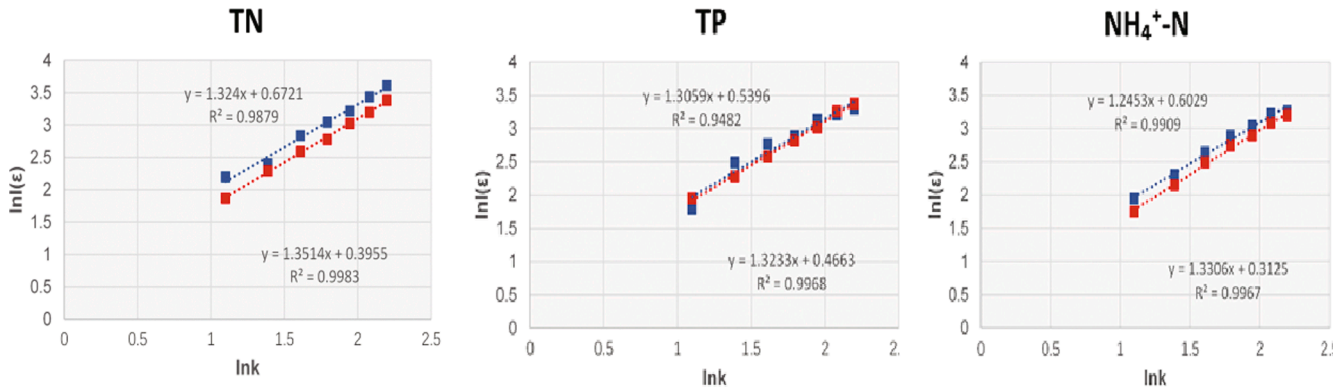

Fig. 8. Capacity dimension of water quality exceeding grade III standards and information dimension of water quality exceeding grade III standards.

reaches of the river. However, information dimension D_I ranges from 1.323 to 1.351 (Fig. 8 and ST4 to ST6). The value of D_0 is less than the D_I, which demonstrated that these points are not spatial distributed equally and therefore the spatial structure presents a complicated characteristic and confirms the fractal phenomenon of local aggregation around main cities and the concentration of farmland and livestock areas, which reflects the process of self-organizing evolution. We also found that the hotspots of N and P loads (see Fig. 4.) are spatially co-located with the catchments of heavily polluted rivers. The middle and upper reaches are densely populated, and the water quality pollution comes from the excessive use of chemical fertilizer, sewage discharge, mining and other agricultural non-point source pollution, sewage discharge in daily life and urban landfill, etc. However, the lower reaches of the WRB represent a relatively primitive ecological environment with extensive forest and extremely low population density. In addition, the economy in these areas is less buoyant and sewage treatment facilities are lacking, which results in most sewage being discharged directly into the river. Water quality impacts are mainly attributed to the cumulative effects of the southeast of upper reaches and southwest of middle reaches; the lower reach areas have fewer reservoirs and the higher river flow leads to the transport of highly polluted loads (Dai et al., 2021), which can clarify the poor water quality in some areas of low reaches (e. g. Furong river watershed). Due to the poor surface water-holding capacity in karst terrain, many small impounded projects in the WRB have been promoted to meet demands for water resource allocation and flood control (Li et al., 2016). According to the Bureau of Hydrology and Resources of Guizhou Province, besides a dam cascade, there are 19,652 small reservoirs in the entire WRB (Dai, 2019). Dam cascade and small reservoirs have altered the hydrological regime, river morphology and lateral connectivity and increased longitudinal fragmentation of the basin (Viaroli et al., 2018), which has further amplified the instability of the biogeochemical processes and extended the range of resulting environment damage. These structural modifications have also increased regional hydraulic retention times and slowed down the flow rate of rivers, in turn hindering river metabolism, amplifying nutrient transport and delivery, but also triggering eutrophication in rivers themselves (Dodds, 2006; Pinay et al., 2002; Viaroli et al., 2018). These geographical characteristics of the WRB and human disturbance factors lead to serious water quality pollution and complications in environment responses in karst areas.

3.5. Uncertainty analysis

Our study mainly focuses on uncertainties associated with model input data and calculation parameters. Sensitivity analysis was conducted (Hong et al., 2013). The most sensitive components of NANI and NAPI are fertilizer inputs, food and feed imports and sewage treatment rate (see SFig. 4). Thus, these parameters were supposed to fluctuate within a range of 10%. In addition, these parameters are supposed to be independent and follow a uniform distribution. So, we chose Monte Carlo sampling to randomly sample 1000 sets of parameters. The results show that the fluxes of N and P in the whole basin varies from 14981.32 $\pm$ 3011.17 to 8775.31 $\pm$ 2213.15 kg N km^{-2} yr^{-1} and 4153.11 $\pm$ 1063 to 3931 + 1213.15 kg P km^{-2} yr^{-1}, the uncertainty of the input loads of N and P in different sub-basin is shown in Fig. 10. The sub-basin with larger input loads of N and P has greater uncertainty, so the uncertainty of N and P load gradually increases from upstream to downstream. There is also uncertainty in N and P loads related to fertilization and agricultural production. The N and P load uncertainty of seven sub-basins varies due to differentiated geographical features and locations, and varying economic development levels (Figs. 9 and 10). The sub-basins with large uncertainties are mainly distributed in the downstream areas, for instance Liuchong and Miaotiao sub-basins.

3.6. Pollutant management challenges in Wu jiang river basin

Guizhou is one of the poorest provinces in China, but it has also one of the fastest economic growth rates in China. Between 2000 and 2018, it experienced rapid economic growth and its GDP growth increased by a factor of 8 from 9.9 trillion yuan to 81.8 trillion yuan. In the future, population pressure, market-oriented agriculture structural changes, urbanization, ecological engineering projects, and broad & strict environmental management policies will lead to greater complexity and unpredictability of variations in artificial N and P loads in the WRB. China's economic support policy to the western region and the recent topical discussion surrounding the 'three-child' policy has seen the total population of the WRB rise with suggestions that this trend will continue. Moreover, the WRB has a large rural population base but limited arable land. This region needs to balance the trade-offs between ensuring food security and promoting economic development, and thus the inputs of N and P may be acute. In the Fourteenth five-year plan of Guizhou province, the local government strongly promoted farming and animal husbandry in order to develop modern and highly efficient agriculture, which further supports the development of mountainous agriculture. In the Guizhou province, agriculture is experiencing change, with subsistence farming giving way to expansion of planting of commercial crops prompted by demands of economic development (Chadwick et al., 2015; Fu et al., 2010). Local government has also been promoting the implementation of the pig subsidy policy and local banks provide opportunities to lend commercial loans to small farmers in Guizhou province. A World Bank-financed project has supported regional development and poverty reduction in rural areas of Guizhou province by organizing small-scale farmers into cooperatives and integrating them to the agricultural value chains (The World Bank, 2016). Intensive agriculture has therefore become a growing trend of rural development in southwest China. Estimates suggest that large-scale production rate of animal husbandry will rise 20%-30% by 2025 (GZPC, 2021). This will likely lead to increased farm size and greater risk

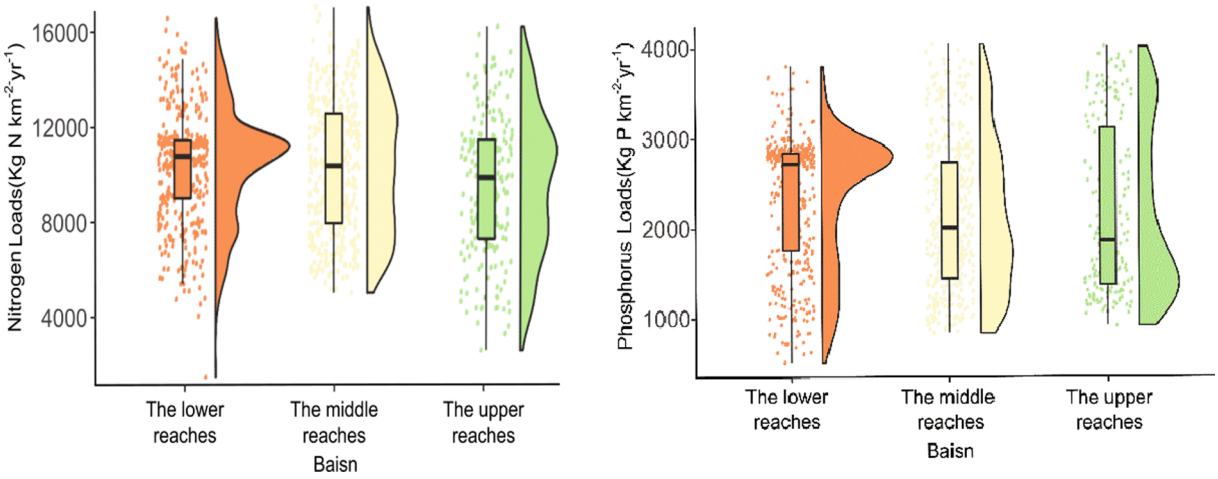

Fig. 9. Uncertainty analysis results of N and P loads in Wu jiang Basin under different reaches.

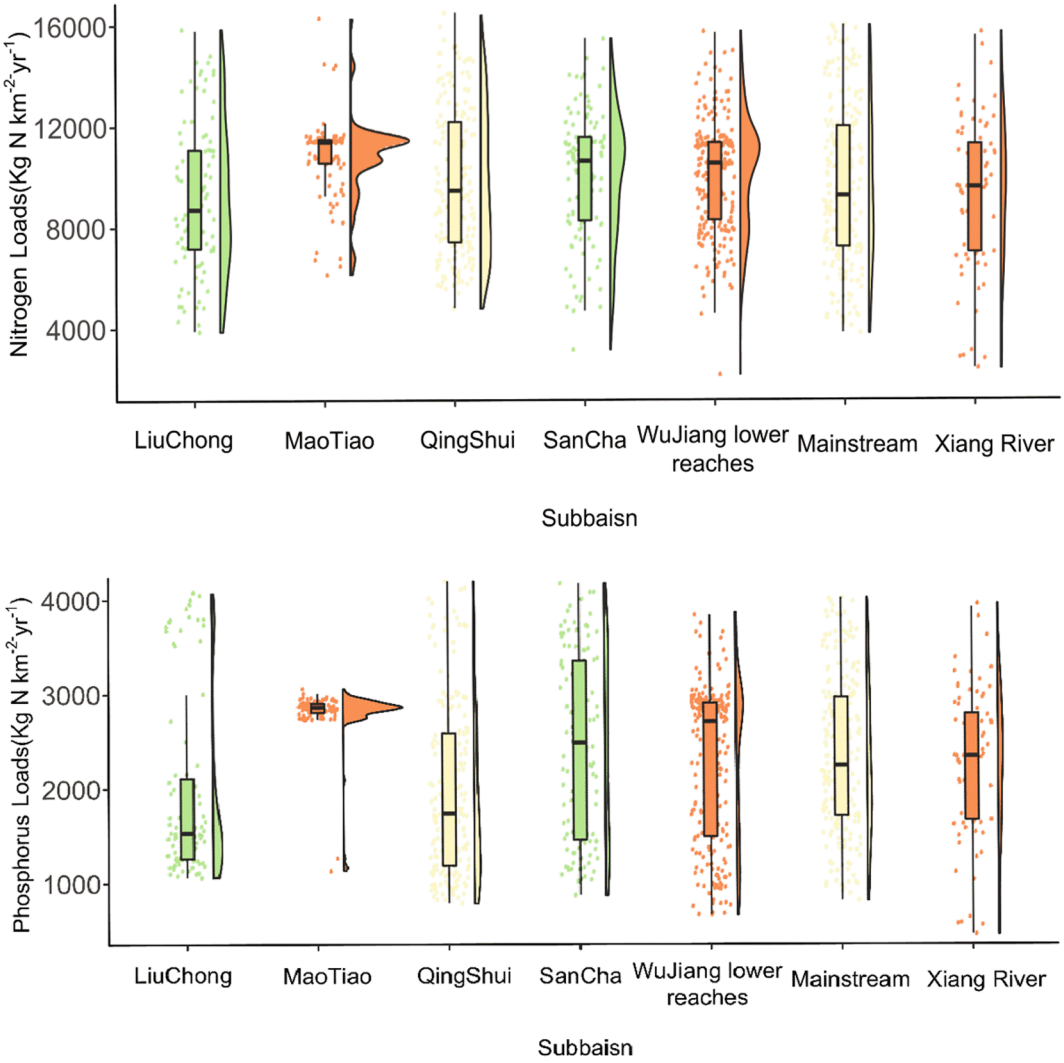

Fig. 10. Uncertainty analysis results of N and P loads in Wu jiang Basin in basins and sub-basins.

of pollution from pesticides, faecal bacteria and metals from animal waste contained in runoff, especially in the karst regions with a high degree of surface–groundwater interaction (Mahler et al., 2021; Mahler et al., 1999; Pan et al., 2017; Buckerfield et al., 2019).

It is claimed that the target for the use synthetic fertilizer in agricultural production has already been achieved by 2020 under the national regulations, but socioeconomic determinants alongside agricultural subsidies result in ambiguous attitudes concerning synthetic

fertilizer use among farmers (Oliver et al., 2020; Smith and Siciliano, 2015). Due to the availability of subsidized synthetic fertilizers, synthetic nitrogen use was still 30.5 Mt in 2016 (Yu et al., 2019b). While fertilizer use has been increasing in the WRB, manure application is likely to increase as farmers will need to source more nutrients from organic fertilizer (Buckerfield et al., 2019). However, optimum management of manure applications to crops is often limited by labor availability, meaning that water pollution issues in Chinese agro-ecosystem frequently arise (Chadwick et al., 2015; Oliver et al., 2020; Smith and Siciliano, 2015).

However, there is evidence that farm communities do consider wider environment consequences alongside their livelihoods, but that the application of manure nutrient sources is often made without adequate knowledge of associated nutrient content and results in application rates far in excess of crop requirements (Oliver et al., 2020). Agricultural advisory services are often limited and this situation is particularly serious in the southwest China karst region (Oliver et al., 2020; Pan et al., 2017; Zheng et al., 2019). Consequently, residual fertility has increased, and so has N and P leaching from the soil environment. Poor farming decisions also promote environment hazards e.g. land degradation, soil erosion and water contamination with consequences for livelihoods (Oliver et al., 2020; Wang et al., 2019). In southwestern China, rocky desertification is considered a serious environmental hazard and a critical hindrance for local agricultural and economic development in this region (Li et al., 2021a). Chinese governments at various levels have initiated ecological engineering projects (e.g., fertilizer used for agriculture and ecological restoration) to manage the trade-offs between agricultural sustainability and ecosystem stability.

3.7. Regional environmental management in Wu jiang river basin

The WRB represents a traditional agricultural area which is transforming to intensive agricultural production. Due to extensive and inefficient nutrient management in the WRB, the land–water system may be trapped in a state of high N and P inputs for a long time. Promoting effective agricultural management and improving nutrient use efficiency are key controls measures to alleviate and potentially reverse the poor water quality trends in this region, which is especially important as a response to the "ecological protection and high-quality development in the Yangtze River basin" (YRCC). Key recommendations include, but are not limited to the following: large-scale ruminant and non-ruminant livestock and poultry breeding should be managed carefully to deliver efficiencies in nutrient management in karst areas to help control farming pollution. Promoting improved knowledge around issues of animal feeding and manure management is also a major direction for effort to reduce excessive N and P emissions, as direct manure inputs to water is a common practice, especially in the rural areas of southwest China (Oliver et al., 2020; Strokal et al., 2016; Zheng et al., 2019). Therefore, promoting a circular economy to capitalize on, e.g. biogas potential, waste residue to return to the field, the manufacture of renewable feed and organic fertilizer etc., will be important to improve the environment in the WRB. Composting technology could be easily implemented to help manage animal manure, with composted manure then used as soil amendment and fertilizer (Dróżdż et al., 2020; Posmanik et al., 2013). Unbalanced nutrient proportions in compound fertilizers can lead to soil acidification, secondary salinization and reduced microbial activity, which reduces yields and may lead farmers to apply more fertilizers to try to compensate for the loss of soil productivity. The soil N and P stock and nutrient mass balance (NMB) calculator are thus advocated in order to compute the N and P imported onto and exported from the farm, which will be beneficial for enhancing nutrient use efficiency (Hobbie et al., 2017). Encouraging the use of fecal energy reuse technology, e.g. anaerobic digestion and pyrolysis in WRB, would also be advantageous for the treatment of animal manure in developed eastern region (Mao et al., 2021).

Combined with policy tools, such as elevating the cost or cancelling the subsidies for synthetic fertilizer production, should result in management changes (Zhang et al., 2019b). Despite it being heavily subsidized by the government, a survey in a small watershed within the WRB showed that 77% of all farmers interviewed identified fertilizer as the most expensive component of their farming activity (Oliver et al., 2020). Improving knowledge about agricultural management and environmental awareness among village communities might be particularly crucial in the WRB rather than simply cancelling the subsides. Given the fact that over 500 million people live in rural areas considered essential for agricultural production in China (Li et al., 2019) the Government should strongly encourage farmers in the WRB to receive multiple sources of training in fertilizer use and manure management via the agricultural extension services (Yang and Fang, 2015), which will likely help to decrease fertilizer use amongst farmers in China.

4. Conclusion

Through past decades, the WRB has been susceptible to water quality impairments induced by high economic growth. Mitigation and management are challenging due to geographical conditions, population pressures, and land-use regimes. Our study provides a fine scale spatio-temporal accounting of human-induced N and P loads in the WRB, the largest karst basin in the world. The research also explored determinants responsible for N and P loads in terms of social and agricultural factors. County level NANI and NAPI has increased from average values of 11,262.06 ± 2732.11 kg N km $^{-2}$ yr^{-1} to 8,653.91 ± 1863.32 kg N km^{-2} yr^{-1} and 3,428.11 ± 1,653.18 kg P km^{-2} yr^{-1} to 3,428.12 ± 1,653.45 kg P km^{-2} yr^{-1} during 2000 to 2018 (almost an increase of 50%).

By performing the GDM, the 8 driving factors discussed in our research all have major implications on N and P loads. Population density has the greatest power to explain N and P pollution, followed by cultivated land, livestock numbers, fertilizer application rates and food production. However, the impact of fertilizer application and food production on nutrient inputs follow a rising trend first, before the impact switches to a declining trend during the study period, while the impact of sewage treatment rate and GDP demonstrates a significant positive relationship with nutrient inputs. Our study helps to underpin the development of effective nutrient management strategies from quantitative and spatially distributed information in karst basins, where more industrial breeding farms are likely to emerge in response to rising population trends and increased animal waste production (associated with increased demand for meat). In ecologically fragile karst areas, to achieve benignant agricultural development while protecting the water environment, it is necessary to formulate long-term coordinated plans among stakeholders and government departments under a unified scientific framework. We advocate reasonable land use planning and effective fertilizer use policies to improve the efficiency of nutrient use, while reducing point source pollution from industry and household emissions, improving sewage treatment capacity, and reducing food and energy waste. At the same time, we highlight that the spillover effects of environmental pollution should be taken account into when conducting pollution control. Furthermore, promoting strict environmental regulations only in hotspot areas will be ineffective and we therefore advocate regional linkages of environmental regulation to deal with climate change and economic development at different stages, which also forms part of an assessment of future nutrient reduction strategies or land use changes. This can serve to help water manager develop region-specific long-term strategies to mitigate nitrogen and phosphorus pollution in severely impaired water bodies, and provide estimates of the water quality benefits likely to be achieved by such management action.

CRediT authorship contribution statement

Guoyu Xu: Conceptualization, Methodology, Software, Validation, Formal analysis, Investigation, Data curation, Writing – original draft,

Visualization. **Jie Xiao:** Conceptualization, Methodology, Software, Validation, Formal analysis, Investigation, Data curation, Writing – original draft, Visualization. **David M. Oliver:** Conceptualization, Writing – review & editing, Supervision. **Zhiqi Yang:** Software, Validation. **Kangning Xiong:** Investigation, Project administration, Funding acquisition. **Zhongming Zhao:** Software, Validation. **Lilin Zheng:** Data curation. **Hongxiang Fan:** Software, Validation, Investigation, Project administration, Funding acquisition. **Fuxiang Zhang:** Data curation.

Declaration of Competing Interest

The authors declare that they have no known competing financial interests or personal relationships that could have appeared to influence the work reported in this paper.

Acknowledgments

This work was supported by the China Overseas Expertise Introduction Program for Discipline Innovation (No. D17016), the Project of Science and Technology Program of Guizhou Province (No. 5411 2017 Qiankehe Pingtai Rencai), the World Top Discipline Program of Guizhou Province (No.125 2019 Qianjiao Keyan Fa), Nanjing Institute of Geography & Limnology (NIGLAS2019QD005), National Natural Science Foundation of China(42001109) and Natural Science Foundation of Jiangsu Province (BK20201102).

Appendix A. Supplementary data

Supplementary data to this article can be found online at https://doi.org/10.1016/j.ecolind.2021.108453.

References

Allan, J.D., Castillo, M.M., Capps, K.A., 2020. Stream ecology: structure and function of running waters. Springer Nature.

Arhonditsis, G.B., Qian, S.S., Stow, C.A., Lamon, E.C., Reckhow, K.H., 2007. Eutrophication risk assessment using Bayesian calibration of process-based models: Application to a mesotrophic lake. Ecol. Model. 208 (2-4), 215–229.

Brooks, B.W., Lazorchak, J.M., Howard, M.D.A., Johnson, M.-V., Morton, S.L., Perkins, D. A.K., Reavie, E.D., Scott, G.I., Smith, S.A., Steevens, J.A., 2016. Are harmful algal blooms becoming the greatest inland water quality threat to public health and aquatic ecosystems? Environ. Toxicol. Chem. 35 (1), 6–13.

Buckerfield, S.J., Waldron, S., Quilliam, R.S., Naylor, L.A., Li, S., Oliver, D.M., 2019. How can we improve understanding of faecal indicator dynamics in karst systems under changing climatic, population and land use stressors? – research opportunities in SW China. Sci. Total Environ. 646, 438–447.

Carpenter, S.R., 2005. Eutrophication of aquatic ecosystems: bistability and soil phosphorus. Proc. Natl. Acad. Sci. 102 (29), 10002–10005.

Chadwick, D., Jia, W., Tong, Y.A., Yu, G.H., Shen, Q.R., Chen, Q., 2015. Improving manure nutrient management towards sustainable agricultural intensification in China. Agr. Ecosyst. Environ. 209, 34–46.

Cheng, D., Li, X., 2020. Relationship between population distribution and topography of theWujiang RiverWatershed in Guizhou province. Geogr. Res. 39 (6), 1427–1438 (In Chinese).

Chen, Z., Auler, A.S., Bakalowicz, M., Drew, D., Griger, F., Hartmann, J., Jiang, G., Moosdorf, N., Richts, A., Stevanovic, Z., Veni, G., Goldscheider, N., 2017. The World Karst Aquifer Mapping project: concept, mapping procedure and map of EuropeDas Welt-Karstaquifer-Kartierprojekt: Konzept, Vorgehensweise und EuropakarteLe programme de la Carte Mondiale des Aquifères Karstiques: concept, procédure de cartographie et carte de l'EuropeMapping: concepto, procedimiento de mapeo y mapa de Europa世界岩溶含水层分布图:制图的概念、流程以及欧洲地区样图Projeto Mapeamento Global de Aquíferos Cársticos (WOKAM): conceito, procedimentos adotados e mapa da Europa. Hydrogeol. J. 25 (3), 771–785.

Cui, M., Guo, Q., Wei, R., Chen, T., 2021a. Temporal-spatial dynamics of anthropogenic nitrogen inputs and hotspots in a large river basin. Chemosphere 269, 129411. https://doi.org/10.1016/j.chemosphere.2020.129411.

Cui, M., Guo, Q., Wei, R., Tian, L., 2021b. Human-driven spatiotemporal distribution of phosphorus flux in the environment of a mega river basin. Sci. Total Environ. 752, 141781. https://doi.org/10.1016/j.scitotenv.2020.141781.

Cui, M., Guo, Q., Wei, R., Wei, Y., 2021c. Anthropogenic nitrogen and phosphorus inputs in a new perspective: Environmental loads from the mega economic zone and city clusters. J. Cleaner Prod. 283, 124589. https://doi.org/10.1016/j.jclepro.2020.124589.

Dai, Y., Lang, Y., Wang, T., Han, X., Wang, L., Zhong, J., 2021. Modelling the sources and transport of ammonium nitrogen with the SPARROW model: A case study in a karst basin. J. Hydrol. 592, 125763. https://doi.org/10.1016/j.jhydrol.2020.125763.

Deng, M., Liu, L., Sun, Z., Piao, S., Ma, Y., Chen, Y., Wang, J., Qiao, C., Wang, X., Li, P., 2016. Increased phosphate uptake but not resorption alleviates phosphorus deficiency induced by nitrogen deposition in temperate Larix principis-rupprechtii plantations. New Phytol. 212 (4), 1019–1029.

Deng, C., Liu, L., Peng, D., Li, H., Zhao, Z., Lyu, C., Zhang, Z., 2021. Net anthropogenic nitrogen and phosphorus inputs in the Yangtze River economic belt: spatiotemporal dynamics, attribution analysis, and diversity management. J. Hydrol. 597, 126221. https://doi.org/10.1016/j.jhydrol.2021.126221.

Diaz, R.J., 2001. Overview of hypoxia around the world. J. Environ. Qual. 30 (2), 275–281.

Ding, X., Shen, Z., Hong, Q., Yang, Z., Wu, X., Liu, R., 2010. Development and test of the Export Coefficient Model in the Upper Reach of the Yangtze River. J. Hydrol. 383 (3-4), 233–244.

Dodds, W.K., 2006. Eutrophication and trophic state in rivers and streams. Limnol. Oceanogr. 51 (1part2), 671–680.

Dróżdż, D., Wystalska, K., Malińska, K., Grosser, A., Grobelak, A., Kacprzak, M., 2020. Management of poultry manure in Poland – Current state and future perspectives. J. Environ. Manage. 264, 110327. https://doi.org/10.1016/j.jenvman.2020.110327.

Dai, Y.B. Yang J., 2019. Estimating the source, distribution, and. transport of the ammonium nitrogen in the Wujiang River Basin based on the SPARROW mode (Master Thesis). Tianjing University, Tianjing, China.

Ford, D., Williams, P., 2007. Karst Hydrogeology and Geomorphology.

Fowler, D., Coyle, M., Skiba, U., Sutton, M.A., Cape, J.N., Reis, S., Sheppard, L.J., Jenkins, A., Grizzetti, B., Galloway, J.N., Vitousek, P., Leach, A., Bouwman, A.F., Butterbach-Bahl, K., Dentener, F., Stevenson, D., Amann, M., Voss, M., 2013. The global nitrogen cycle in the twenty-first century. Philos. Trans. Royal Soc. B: Biol. Sci. 368 (1621), 20130164.

Frankhauser, P., 1998. The fractal approach. A new tool for the spatial analysis of urban agglomerations. Population 205–240.

Ford, A., Blenkinsop, T.G., 2008. Combining fractal analysis of mineral deposit clustering with weights of evidence to evaluate patterns of mineralization: Application to copper deposits of the Mount Isa Inlier, NW Queensland, Australia. Ore Geol. Rev. 33 (3-4), 435–450.

Fiorillo, Francesco, Pagnozzi, Mauro, Ventafridda, Gerardo, 2015. A model to simulate recharge processes of karst massifs. Hydrol. Process. 29 (10), 2301–2314.

Gao, Wei, Howarth, Robert W., Swaney, Dennis P., Hong, Bongghi, Guo, Huai Cheng, 2015. Enhanced N input to Lake Dianchi Basin from 1980 to 2010: Drivers and consequences. Sci. Total Environ. 505, 376–384.

Garg, A., Agrawal, A., Negi, A., 2014. A Review on Natural Phenomenon of Fractal Geometry. Int. J. Comput. Applications 86, 975–8887.

Goyette, Jean-Olivier, Bennett, Elena M., Maranger, Roxane, 2019. Differential influence of landscape features and climate on nitrogen and phosphorus transport throughout the watershed. Biogeochemistry 142 (1), 155–174.

Goyette, J.O., Bennett, E.M., Howarth, R.W., Maranger, R., 2016. Changes in anthropogenic nitrogen and phosphorus inputs to the St. Lawrence sub-basin over 110years and impacts on riverine export. Global Biogeochem. Cycles 30 (7), 1000–1014.

Guignard, M.S., Leitch, A.R., Acquisti, C., Eizaguirre, C., Elser, J.J., Hessen, D.O., Jeyasingh, P.D., Neiman, M., Richardson, A.E., Soltis, P.S., Soltis, D.E., Stevens, C.J., Trimmer, M., Weider, L.J., Woodward, G. and Leitch, I.J. (2017) Impacts of Nitrogen and Phosphorus: From Genomes to Natural Ecosystems and Agriculture. Front. Ecol. Evol. 5.

GZPC, 2021. The People's Government of Guizhou Province: The Fourteenth Five-Year Plan for the National Economic and Social Development of Guizhou Province and the Outline of 2035 Long-range Goals. http://fgw.guizhou.gov.cn/.

Hashemi, Fatemeh, Olesen, Jørgen E., Dalgaard, Tommy, Børgesen, Christen D., 2016. Review of scenario analyses to reduce agricultural nitrogen and phosphorus loading to the aquatic environment. Sci. Total Environ. 573, 608–626.

Han, Haejin, Allan, J. David, 2008. Estimation of nitrogen inputs to catchments: Comparison of methods and consequences for riverine export prediction. Biogeochemistry 91 (2-3), 177–199.

Han, Yuguo, Fan, Yuntao, Yang, Peiling, Wang, Xiaoxue, Wang, Yujie, Tian, Jinxia, Xu, Lei, Wang, Chengzhi, 2014. Net anthropogenic nitrogen inputs (NANI) index application in Mainland China. Geoderma 213, 87–94.

Han, Yuguo, Yu, Xinxiao, Wang, Xiaoxue, Wang, Yunqi, Tian, Jinxia, Xu, Lei, Wang, Chengzhi, 2013. Net anthropogenic phosphorus inputs (NAPI) index application in Mainland China. Chemosphere 90 (2), 329–337.

Harrison, John A., Maranger, Roxane J., Alexander, Richard B., Giblin, Anne E., Jacinthe, Pierre-Andre, Mayorga, Emilio, Seitzinger, Sybil P., Sobota, Daniel J., Wollheim, Wilfred M., 2009. The regional and global significance of nitrogen removal in lakes and reservoirs. Biogeochemistry 93 (1-2), 143–157.

Hartmann, A., Gleeson, T., Rosolem, R., Pianosi, F., Wada, Y., Wagener, T., 2015. A large-scale simulation model to assess karstic groundwater recharge over Europe and the Mediterranean. Geosci. Model Dev. 8 (6), 1729–1746.

Hartmann, A., Goldscheider, N., Wagener, T., Lange, J., Weiler, M., 2014. Karst water resources in a changing world: Review of hydrological modeling approaches. Rev. Geophys. 52 (3), 218–242.

Hobbie, S., Finlay, J., Janke, B., Nidzgorski, D., Millet, D., Baker, L., 2017. Contrasting nitrogen and phosphorus budgets in urban watersheds and implications for managing urban water pollution. Proc. Natl. Acad. Sci. U.S.A. 114.

Hong, B., Swaney, D.P., Howarth, R.W., 2013. Estimating Net Anthropogenic Nitrogen Inputs to U.S. Watersheds: Comparison of Methodologies. Environ. Sci. Technol. 47 (10), 5199–5207.

Hong, Bongghi, Swaney, Dennis P., McCrackin, Michelle, Svanbäck, Annika, Humborg, Christoph, Gustafsson, Bo, Yershova, Alexandra, Pakhomau, Aliaksandr, 2017. Advances in NANI and NAPI accounting for the Baltic drainage basin: spatial

and temporal trends and relationships to watershed TN and TP fluxes. Biogeochemistry 133 (3), 245–261.
Hong, Bongghi, Swaney, Dennis P., Mörth, Carl-Magnus, Smedberg, Erik, Eriksson Hägg, Hanna, Humborg, Christoph, Howarth, Robert W., Bouraoui, Fayçal, 2012. Evaluating regional variation of net anthropogenic nitrogen and phosphorus inputs (NANI/NAPI), major drivers, nutrient retention pattern and management implications in the multinational areas of Baltic Sea basin. Ecol. Model. 227, 117–135.
Howarth, Robert, Swaney, Dennis, Billen, Gilles, Garnier, Josette, Hong, Bongghi, Humborg, Christoph, Johnes, Penny, Mörth, Carl-Magnus, Marino, Roxanne, 2012. Nitrogen fluxes from the landscape are controlled by net anthropogenic nitrogen inputs and by climate. Front. Ecol. Environ. 10 (1), 37–43.
Howarth, R.W., Billen, G., Swaney, D., Townsend, A., Jaworski, N., Lajtha, K., Downing, J.A., Elmgren, R., Caraco, N., Jordan, T., Berendse, F., Freney, J., Kudeyarov, V., Murdoch, P., Zhao-Liang, Z., 1996. Regional nitrogen budgets and riverine N & P fluxes for the drainages to the North Atlantic Ocean: Natural and human influences. Biogeochemistry 35 (1), 75–139.
Huang, H., Chen, D.J., Zhang, B.F., Zeng, L.Z., Dahlgren, R.A., 2014. Modeling and forecasting riverine dissolved inorganic nitrogen export using anthropogenic nitrogen inputs, hydroclimate, and land-use change. J. Hydrol. 517, 95–104.
Jiang, Z., Lian, Y., Qin, X., 2014. Rocky desertification in Southwest China: Impacts, causes, and restoration. Earth Sci. Rev. 132, 1–12.
Jing, W.E.I., Lin, M.A., Guang, L.U., WenQi, M.A., JianHui, L.I., Lu, Z., 2008. The influence of urbanization on nitrogen flow and recycling utilization in food consumption system of China. Acta Ecologica Sinica 28 (3), 1016–1025 (in Chinese).
Kunz, Manuel J., Anselmetti, Flavio S., Wüest, Alfred, Wehrli, Bernhard, Vollenweider, Adrian, Thüring, Silvan, Senn, David B., 2011. Sediment accumulation and carbon, nitrogen, and phosphorus deposition in the large tropical reservoir Lake Kariba (Zambia/Zimbabwe). J. Geophys. Res. Biogeosci. 116 (G3) https://doi.org/10.1029/2010JG001538.
Li, Si-Liang, Liu, Cong-Qiang, Chen, Jin-An, Wang, Shi-Jie, 2021a. Karst ecosystem and environment: Characteristics, evolution processes, and sustainable development. Agric. Ecosyst. Environ. 306, 107173. https://doi.org/10.1016/j.agee.2020.107173.
Li, Yurui, Fan, Pengcan, Liu, Yansui, 2019. What makes better village development in traditional agricultural areas of China? Evidence from long-term observation of typical villages. Habitat Int. 83, 111–124.
Li, Zhenwei, Xu, Xianli, Yu, Bofu, Xu, Chaohao, Liu, Meixian, Wang, Kelin, 2016. Quantifying the impacts of climate and human activities on water and sediment discharge in a karst region of southwest China. J. Hydrol. 542, 836–849.
Li, Ji, Hong, Aihua, Yuan, Daoxian, Jiang, Yongjun, Deng, Shujin, Cao, Cong, Liu, Jiao, 2021b. A new distributed karst-tunnel hydrological model and tunnel hydrological effect simulations. J. Hydrol. 593, 125639. https://doi.org/10.1016/j.jhydrol.2020.125639.
MacDonald, G.K., Bennett, E.M., Potter, P.A., Ramankutty, N., 2011. Agronomic phosphorus imbalances across the world's croplands. Proc. Natl. Acad. Sci. 108 (7), 3086–3091.
FNPSC (First National Pollution Source Census), 2010. http://cpsc.mep.gov.cn/ (last access: 01.08.2018).
Mahler, Barbara J., Jiang, Yongjun, Pu, Junbing, Martin, Jonathan B., 2021. Editorial: Advances in hydrology and the water environment in the Karst Critical Zone under the impacts of climate change and anthropogenic activities. J. Hydrol. 595, 125982. https://doi.org/10.1016/j.jhydrol.2021.125982.
Mahler, B.J., Lynch, L., Bennett, P.C., 1999. Mobile sediment in an urbanizing karst aquifer: implications for contaminant transport. Environ. Geol. 39 (1), 25–38.
Malagò, Anna, Efstathiou, Dionissios, Bouraoui, Fayçal, Nikolaidis, Nikolaos P., Franchini, Marco, Bidoglio, Giovanni, Kritsotakis, Marinos, 2016. Regional scale hydrologic modeling of a karst-dominant geomorphology: The case study of the Island of Crete. J. Hydrol. 540, 64–81.
Mao, Yupeng, Zhang, Hong, Tang, Wenzhong, Zhao, Jianwei, Wang, Zhipeng, Fan, Aoxiang, 2021. Net anthropogenic nitrogen and phosphorus inputs in Pearl River Delta region (2008–2016). J. Environ. Manage. 282, 111952. https://doi.org/10.1016/j.jenvman.2021.111952.
Marsiglio, Simone, Ansuategi, Alberto, Gallastegui, Maria Carmen, 2016. The Environmental Kuznets Curve and the Structural Change Hypothesis. Environ. Resour. Econ. 63 (2), 265–288.
Martínez-Sabater, E., García-Muñoz, M., Bonete, P., Rodriguez, M., Sánchez-García, F.B., Pérez-Murcia, M.D., Bustamante, M.A., López-Lluch, D.B., Moral, R., 2019. Comprehensive management of dog faeces: Composting versus anaerobic digestion. J. Environ. Manage. 250, 109437. https://doi.org/10.1016/j.jenvman.2019.109437.
Mayorga, Emilio, Seitzinger, Sybil P., Harrison, John A., Dumont, Egon, Beusen, Arthur H.W., Bouwman, A.F., Fekete, Balazs M., Kroeze, Carolien, Van Drecht, Gerard, 2010. Global nutrient export from WaterSheds 2 (NEWS 2): model development and implementation. Environ. Modell. Software 25 (7), 837–853.
Metson, Genevieve S., Lin, Jiajia, Harrison, John A., Compton, Jana E., 2017. Linking terrestrial phosphorus inputs to riverine export across the United States. Water Res. 124, 177–191.
Nesme, Thomas, Metson, Geneviève S., Bennett, Elena M., 2018. Global phosphorus flows through agricultural trade. Global Environ. Change 50, 133–141.
Oliver, David M, Zheng, Ying, Naylor, Larissa A., Murtagh, Madeleine, Waldron, Susan, Peng, Tao, 2020. How does smallholder farming practice and environmental awareness vary across village communities in the karst terrain of southwest China? Agriculture. Ecosyst. Environ. 288, 106715. https://doi.org/10.1016/j.agee.2019.106715.
Pan, Dan, Kong, Fanbin, Zhang, Ning, Ying, Ruiyao, 2017. Knowledge training and the change of fertilizer use intensity: Evidence from wheat farmers in China. J. Environ. Manage. 197, 130–139.
Pinay, Gilles, Clément, Jean Christophe, Naiman, Robert J., 2002. Basic Principles and Ecological Consequences of Changing Water Regimes on Nitrogen Cycling in Fluvial Systems. Environ. Manage. 30 (4), 481–491.
Porter, Ellen M., Bowman, William D., Clark, Christopher M., Compton, Jana E., Pardo, Linda H., Soong, Jenny L., 2013. Interactive effects of anthropogenic nitrogen enrichment and climate change on terrestrial and aquatic biodiversity. Biogeochemistry 114 (1-3), 93–120.
Posmanik, Roy, Nejidat, Ali, Bar-Sinay, Boaz, Gross, Amit, 2013. Integrated biological treatment of fowl manure for nitrogen recovery and reuse. J. Environ. Manage. 117, 172–179.
Powers, Stephen M., Bruulsema, Thomas W., Burt, Tim P., Chan, Neng Iong, Elser, James J., Haygarth, Philip M., Howden, Nicholas J.K., Jarvie, Helen P., Lyu, Yang, Peterson, Heidi M., Sharpley, Andrew N., Shen, Jianbo, Worrall, Fred, Zhang, Fusuo, 2016. Long-term accumulation and transport of anthropogenic phosphorus in three river basins. Nat. Geosci. 9 (5), 353–356.
Qiu, Yong, Shi, Han-chang, He, Miao, 2010. (2010) Nitrogen and Phosphorous Removal in Municipal Wastewater Treatment Plants in China: A Review. Int. J. Chem. Eng. 2010, 1–10.
Rabalais, Nancy N., 2002. Nitrogen in aquatic ecosystems. AMBIO: A Journal of the Human. Environment 31 (2), 102–112.
Regmi, A., Dyck, J., 2001. Effects of urbanization on global food demand. Changing Structure of Global Food Consumption And Trade 23–30.
Regmi, A., Dyck, J., 2001b. Reasons Why Rural and Urban Food Consumption May Differ.
Russell, Marc J., Weller, Donald E., Jordan, Thomas E., Sigwart, Kevin J., Sullivan, Kathryn J., 2008. Net anthropogenic phosphorus inputs: spatial and temporal variability in the Chesapeake Bay region. Biogeochemistry 88 (3), 285–304.
Schaefer, Sylvia C., Hollibaugh, James T., Alber, Merryl, 2009. Watershed nitrogen input and riverine export on the west coast of the US. Biogeochemistry 93 (3), 219–233.
Scholz, Roland W., Wellmer, Friedrich-Wilhelm, 2013. Approaching a dynamic view on the availability of mineral resources: What we may learn from the case of phosphorus? Global Environ. Change 23 (1), 11–27.
Seitzinger, S.P., Harrison, J.A., Dumont, Egon, Beusen, Arthur H.W., Bouwman, A.F., 2005. Sources and delivery of carbon, nitrogen, and phosphorus to the coastal zone: An overview of Global Nutrient Export from Watersheds (NEWS) models and their application. Global Biogeochem. Cycles 19 (4), n/a–n/a.
Singh, Jaswinder, Knapp, H. Vernon., Arnold, J.G., Demissie, Misganaw, 2005. Hydrological modeling of the iroquois river watershed using HSPF and SWAT1. JAWRA J. Am. Water Resour. Assoc. 41 (2), 343–360.
Sinha, Eva, Michalak, Anna M., 2016. Precipitation Dominates Interannual Variability of Riverine Nitrogen Loading across the Continental United States. Environ. Sci. Technol. 50 (23), 12874–12884.
Sinha, E., Michalak, A.M., Calvin, K.V., Lawrence, P.J., 2019. Societal decisions about climate mitigation will have dramatic impacts on eutrophication in the 21st century. Nat. Commun. 10 (1), 939.
Smith, L.E.D., Siciliano, G., 2015. A comprehensive review of constraints to improved management of fertilizers in China and mitigation of diffuse water pollution from agriculture. Agric. Ecosyst. Environ. 209, 15–25.
Sobota, Daniel J, Compton, Jana E, Harrison, John A, 2013. Reactive nitrogen inputs to US lands and waterways: how certain are we about sources and fluxes? Front. Ecol. Environ. 11 (2), 82–90.
Song, Xianwei, Gao, Yang, Green, Sophie M., Wen, Xuefa, Dungait, Jennifer A.J., Xiong, Bailian, Quine, Timothy A., He, Nianpeng, 2019. Rainfall driven transport of carbon and nitrogen along karst slopes and associative interaction characteristic. J. Hydrol. 573, 246–254.
Steffen, W., Richardson, K., Rockström, J., Cornell, S.E., Fetzer, I., Bennett, E.M., Biggs, R., Carpenter, S.R., de Vries, W., de Wit, C.A., Folke, C., Gerten, D., Heinke, J., Mace, G.M., Persson, L.M., Ramanathan, V., Reyers, B., Sörlin, S., 2015. Planetary boundaries: Guiding human development on a changing planet. Science 347 (6223), 1259855.
Strokal, Maryna, Ma, Lin, Bai, Zhaohai, Luan, Shengji, Kroeze, Carolien, Oenema, Oene, Velthof, Gerard, Zhang, Fusuo, 2016. Alarming nutrient pollution of Chinese rivers as a result of agricultural transitions. Environ. Res. Lett. 11 (2), 024014. https://doi.org/10.1088/1748-9326/11/2/024014.
Swaney, D.P., Hong, B., Paneer Selvam, A., Howarth, R.W., Ramesh, R., Purvaja, R., 2015. Net anthropogenic nitrogen inputs and nitrogen fluxes from Indian watersheds: An initial assessment. J. Mar. Syst. 141, 45–58.
The World Bank, 2016. Cooperatives Sow Opportunity for Poor Farmers in China's Guizhou Province. https://www.worldbank.org/en/news/feature/2019/10/11/cooperatives-sow-opportunity-for-poor-farmers-in-chinas-guizhou-province.
Tong, Yindong, Wang, Mengzhu, Peñuelas, Josep, Liu, Xueyan, Paerl, Hans W., Elser, James J., Sardans, Jordi, Couture, Raoul-Marie, Larssen, Thorjørn, Hu, Hongying, Dong, Xin, He, Wei, Zhang, Wei, Wang, Xuejun, Zhang, Yang, Liu, Yi, Zeng, Siyu, Kong, Xiangzhen, Janssen, Annette B.G., Lin, Yan, 2020. Improvement in municipal wastewater treatment alters lake nitrogen to phosphorus ratios in populated regions. Proc. Natl. Acad. Sci. 117 (21), 11566–11572.
Viaroli, Pierluigi, Soana, Elisa, Pecora, Silvano, Laini, Alex, Naldi, Mariachiara, Fano, Elisa Anna, Nizzoli, Daniele, 2018. Space and time variations of watershed N and P budgets and their relationships with reactive N and P loadings in a heavily impacted river basin (Po river, Northern Italy). Sci. Total Environ. 639, 1574–1587.
Vilmin, Lauriane, Flipo, Nicolas, Escoffier, Nicolas, Groleau, Alexis, 2018. Estimation of the water quality of a large urbanized river as defined by the European WFD: what is the optimal sampling frequency? Environ. Sci. Pollut. Res. Int. 25 (24), 23485–23501.

Vitousek, P., Howarth, R., 1991. Nitrogen limitation on land and in the sea: how can it occur? Biogeochemistry 13:87–115. Biogeochemistry 13, 87–115.
Wang, Jin-Feng, Li, Xin-Hu, Christakos, George, Liao, Yi-Lan, Zhang, Tin, Gu, Xue, Zheng, Xiao-Ying, 2010. Geographical detectors-based health risk assessment and its application in the neural tube defects study of the Heshun Region, China. Int. J. Geogr. Inform. Sci. 24 (1), 107–127.
Wang, Kelin, Zhang, Chunhua, Chen, Hongsong, Yue, Yueming, Zhang, Wei, Zhang, Mingyang, Qi, Xiangkun, Fu, Zhiyong, 2019. Karst landscapes of China: patterns, ecosystem processes and services. Landscape Ecol. 34 (12), 2743–2763.
Walsh, Christopher J., Roy, Allison H., Feminella, Jack W., Cottingham, Peter D., Groffman, Peter M., Morgan, Raymond P., 2005. The urban stream syndrome: current knowledge and the search for a cure. J. North Am. Benthol. Soc. 24 (3), 706–723.
Wang, Yang, Wang, Shaojian, Li, Guangdong, Zhang, Hongou, Jin, Lixia, Su, Yongxian, Wu, Kangmin, 2017. Identifying the determinants of housing prices in China using spatial regression and the geographical detector technique. Appl. Geogr. 79, 26–36.
Wang, Jin-Feng, Zhang, Tong-Lin, Fu, Bo-Jie, 2016. A measure of spatial stratified heterogeneity. Ecol. Ind. 67, 250–256.
Yang, L., Chengxin, F.A.N., Lu, Z., 2003. Characteristics of Industrial Wastewater Discharge in a Typical District of Taihu Watershed: A Case Study of Liyang City, Jiangsu Province. J. Lake Sci. 15, 139–146.
Yang, Mengdi, Li, Xiao-Dong, Huang, Jun, Ding, Shiyuan, Cui, Gaoyang, Liu, Cong-Qiang, Li, Qinkai, Lv, Hong, Yi, Yuanbi, 2020. Damming effects on river sulfur cycle in karst area: A case study of the Wujiang cascade reservoirs. Agric. Ecosyst. Environ. 294, 106857. https://doi.org/10.1016/j.agee.2020.106857.
Yang, Xiaoying, Fang, Shubo, 2015. Practices, perceptions, and implications of fertilizer use in East-Central China. Ambio 44 (7), 647–652.
Ye, Xingqing, Christiansen, Flemming, 2009. China's urban-rural integration policies. J. Curr. Chin. Affairs 38 (4), 117–143.
Yu, Guirui, Jia, Yanlong, He, Nianpeng, Zhu, Jianxing, Chen, Zhi, Wang, Qiufeng, Piao, Shilong, Liu, Xuejun, He, Honglin, Guo, Xuebing, Wen, Zhang, Li, Pan, Ding, Guoan, Goulding, Keith, 2019a. Stabilization of atmospheric nitrogen deposition in China over the past decade. Nat. Geosci. 12 (6), 424–429.
Yu, C., Huang, X., Chen, H., Godfray, H.C.J., Wright, J.S., Hall, J.W., Gong, P., Ni, S., Qiao, S., Huang, G., Xiao, Y., Zhang, J., Feng, Z., Ju, X., Ciais, P., Stenseth, N.C., Hessen, D.O., Sun, Z., Yu, L., Cai, W., Fu, H., Huang, X., Zhang, C., Liu, H., Taylor, J., 2019b. Managing nitrogen to restore water quality in China. Nature 567 (7749), 516–520.
Zeng, Jie, Yue, Fu-Jun, Li, Si-Liang, Wang, Zhong-Jun, Qin, Cai-Qing, Wu, Qi-Xin, Xu, Sheng, 2020. Agriculture driven nitrogen wet deposition in a karst catchment in southwest China. Agric. Ecosyst. Environ. 294, 106883. https://doi.org/10.1016/j.agee.2020.106883.
Zhang, Wangshou, Li, Hengpeng, Li, Yunliang, 2019b. Spatio-temporal dynamics of nitrogen and phosphorus input budgets in a global hotspot of anthropogenic inputs. Sci. Total Environ. 656, 1108–1120.
Zhang, W.S., Li, H.P., Kendall, A.D., Hyndman, D.W., Diao, Y.Q., Geng, J.W., Pang, J.P., 2019c. Nitrogen transport and retention in a headwater catchment with dense distibutions of lowland ponds. Sci. Total Environ. 683, 37–48.
Zhang, X., Davidson, E.A., Zou, T., Lassaletta, L., Quan, Z., Li, T., Zhang, W., 2020. Quantifying Nutrient Budgets for Sustainable Nutrient Management. Glob. Biogeochem. Cycles 34(3), e2018GB006060.
Zhang, xinping, li, l., chen, x.p., shuo, Z., 2009. The development status and existing problems of compound fertilizer in China (in Chinese).
Zheng, Ying, Naylor, Larissa A., Waldron, Susan, Oliver, David M., 2019. Knowledge management across the environment-policy interface in China: What knowledge is exchanged, why, and how is this undertaken? Environ. Sci. Policy 92, 66–75.